

ON THE MULTIPLICITY OF PERIODIC ORBITS AND HOMOCLINICS NEAR CRITICAL ENERGY LEVELS OF HAMILTONIAN SYSTEMS IN \mathbb{R}^4

NAIARA V. DE PAULO AND PEDRO A. S. SALOMÃO

ABSTRACT. We study two-degree-of-freedom Hamiltonian systems. Let us assume that the zero energy level of a real-analytic Hamiltonian function $H : \mathbb{R}^4 \rightarrow \mathbb{R}$ contains a saddle-center equilibrium point lying in a strictly convex sphere-like singular subset $S_0 \subset H^{-1}(0)$. From previous work [8] we know that for any small energy $E > 0$, the energy level $H^{-1}(E)$ contains a closed 3-ball S_E in a neighborhood of S_0 admitting a singular foliation called 2 – 3 foliation. One of the binding orbits of this singular foliation is the Lyapunoff orbit $P_{2,E}$ contained in the center manifold of the saddle-center. The other binding orbit lies in the interior of S_E and spans a one parameter family of disks transverse to the Hamiltonian vector field. In this article we show that the 2 – 3 foliation forces the existence of infinitely many periodic orbits and infinitely many homoclinics to $P_{2,E}$ in S_E . Moreover, if the branches of the stable and unstable manifolds of $P_{2,E}$ inside S_E do not coincide then the Hamiltonian flow on S_E has positive topological entropy. We also present applications of these results to some classical Hamiltonian systems.

CONTENTS

1. Introduction	1
2. Main result	2
3. Applications	7
3.1. Buckled nanobeams	8
3.2. The Hénon-Heiles Hamiltonian	10
3.3. Charged particles in planetary magnetospheres	11
4. Existence of a homoclinic to the Lyapunoff orbit	13
5. Infinite twist of the local transition map	15
6. Positive topological entropy	19
7. Area preserving homeomorphisms of the open annulus	23
References	27

1. INTRODUCTION

Various phenomena in nature can be modeled by two-degree-of-freedom Hamiltonian systems. Due to the preservation of energy, one usually restricts the study of the dynamics to a fixed 3-dimensional energy level. Global surfaces of sections, when they exist, provide additional reduction of the flow to an area preserving surface map. When the global surfaces of section are not available, one may still search for the so called systems of transversal sections as introduced by Hofer,

Wysocki and Zehnder in [16]. These systems are singular foliations of the energy level whose singular set is formed by finitely many periodic orbits called bindings. The regular leaves are punctured embedded surfaces foliating the complement of the bindings. They are transverse to the Hamiltonian vector field and are asymptotic to the bindings at the punctures. Systems of transversal sections may determine transition maps between some regular leaves and valuable information about the dynamics may be extracted from standard tools in surface discrete dynamics.

In this paper we study real-analytic Hamiltonian systems in \mathbb{R}^4 admitting a special type of system of transversal sections, the so called 2 – 3 foliation. This is a singular foliation of a closed 3-ball B with precisely two bindings. One of the bindings is hyperbolic and lies in the boundary ∂B . It separates ∂B into two hemispheres which are regular leaves of the foliation. The other binding lies in the interior of B and spans a family of disk-like regular leaves parameterized by an open interval. At the ends of this open interval, the family of disks ‘breaks’ into the union of a cylinder connecting the two bindings and one of the hemispheres of ∂B , depending on the end of the interval, see Figure 2.6 below.

A 2–3 foliation is proved to exist in [8] for small positive energies. More precisely, the zero energy level of the Hamiltonian function is supposed to contain a strictly convex sphere-like singular subset S_0 with a unique singularity corresponding to a saddle-center equilibrium point. Then for every small positive energy, the energy level contains a closed 3-ball S_E in a neighborhood of S_0 and S_E admits a 2 – 3 foliation, see [8, Theorem 1.9]. The binding $P_{2,E} \subset \partial S_E$ coincides with the Lyapunoff orbit in the center manifold of the saddle-center. It has Conley-Zehnder index 2 and represents an obstruction for the existence of a disk-like global surface of section as constructed in [15], see also [18].

The main result in this article asserts that the 2 – 3 foliation obtained in [8] forces the existence of infinitely many periodic orbits and infinitely many homoclinics to $P_{2,E}$ inside S_E . We split the proof in two cases: if the branches of the stable and unstable manifolds of $P_{2,E}$ coincide then part of the dynamics inside S_E is reduced to a homeomorphism of an open punctured disk which preserves a finite area and has infinite twist near the punctures. Infinitely many periodic orbits are thus derived from a generalization of the Poincaré-Birkhoff fixed point theorem due to Franks [9]. If the invariant branches of the stable and unstable manifolds do not coincide then the real-analyticity of the Hamiltonian is used to find infinitely many transverse homoclinics. In particular, there exist horseshoe-type subsystems implying positivity of the topological entropy. Finally, we apply our results to a couple of Hamiltonian systems arising in celestial mechanics and nanotechnology.

2. MAIN RESULT

Let $H : \mathbb{R}^4 \rightarrow \mathbb{R}$ be a real-analytic function. Consider coordinates (x_1, x_2, y_1, y_2) in \mathbb{R}^4 and let

$$\omega_0 = \sum_{i=1,2} dy_i \wedge dx_i$$

be the standard symplectic form. The Hamiltonian vector field associated to H is defined by

$$i_{X_H} \omega_0 = -dH,$$

and so it is given by $X_H = J_0 \nabla H$, where J_0 is the usual symplectic matrix

$$J_0 = \begin{pmatrix} 0 & I_{2 \times 2} \\ -I_{2 \times 2} & 0 \end{pmatrix}$$

and ∇H is the gradient of H .

Let us assume that the energy level $H^{-1}(0)$ contains a saddle-center equilibrium point p_c . This is a critical point of H so that the matrix $J_0 \text{Hess}H(p_c)$ has a pair of real eigenvalues $\pm\alpha$ and a pair of purely imaginary eigenvalues $\pm\omega i$ for some $\alpha, \omega > 0$. Here $\text{Hess}H$ is the Hessian matrix of H .

By a theorem of J. Moser [20] and a refinement of H. Rüssmann [23] (see also Delatte [6]) there exists a real-analytic symplectic change of coordinates $(x_1, x_2, y_1, y_2) = \varphi(q_1, q_2, p_1, p_2) \in \mathbb{R}^4$, defined on neighborhoods $V, U \subset \mathbb{R}^4$ of $0, p_c$, respectively, so that

$$\varphi^* \omega_0 = \sum_{i=1,2} dp_i \wedge dq_i,$$

and, up to adding a constant to H and multiplying it by -1 , the Hamiltonian function $\varphi^* H$ takes the form

$$(2.1) \quad K(q_1, q_2, p_1, p_2) = \bar{K}(I_1, I_2) = -\alpha I_1 + \omega I_2 + R(I_1, I_2),$$

where $I_1 = q_1 p_1$, $I_2 = \frac{q_2^2 + p_2^2}{2}$ and $R(I_1, I_2) = O(I_1^2 + I_2^2)$. According to our conventions, this last identity means that there exists $C > 0$ so that $|R(I_1, I_2)| \leq C(I_1^2 + I_2^2)$ on a small neighborhood of $(0, 0)$. The local coordinates (q_1, q_2, p_1, p_2) near p_c are called Moser's coordinates.

The trajectories of $\dot{z} = J_0 \nabla K(z)$, $z = (q_1, q_2, p_1, p_2)$, are given by

$$(2.2) \quad \begin{cases} q_1(t) = q_1(0)e^{-\alpha t}, \\ p_1(t) = p_1(0)e^{\alpha t}, \\ q_2(t) + ip_2(t) = (q_2(0) + ip_2(0))e^{-i\omega t}, \end{cases}$$

and project to the planes (q_1, p_1) and (q_2, p_2) as in Figure 2.1. Here

$$\begin{aligned} \bar{\alpha}(I_1, I_2) &:= -\partial_{I_1} \bar{K}(I_1, I_2) = \alpha - \partial_{I_1} R(I_1, I_2), \\ \bar{\omega}(I_1, I_2) &:= \partial_{I_2} \bar{K}(I_1, I_2) = \omega + \partial_{I_2} R(I_1, I_2), \end{aligned}$$

are constant along the solutions of (2.2) since I_1 and I_2 are first integrals of the flow.

The projection of the energy levels to the (q_1, p_1) -plane is depicted in Figure 2.2. The critical energy level $K^{-1}(0)$ in these local coordinates projects to the first and third quadrants of the plane (q_1, p_1) . Without loss of generality, we focus on the subset of the critical level projecting to the first quadrant. For all $\delta > 0$ small we let $N_0^\delta \subset K^{-1}(0)$ be the embedded 2-sphere [8, Lemma 1.4] defined by

$$N_0^\delta := K^{-1}(0) \cap \{q_1 + p_1 = \delta\}.$$

Then N_0^δ bounds a topological closed 3-ball $B_0^\delta \subset K^{-1}(0)$ given by

$$B_0^\delta := \bigcup_{0 \leq \epsilon \leq \delta} N_0^\epsilon = K^{-1}(0) \cap \{0 \leq q_1 + p_1 \leq \delta\}.$$

Notice that B_0^δ contains the saddle-center equilibrium as its center.

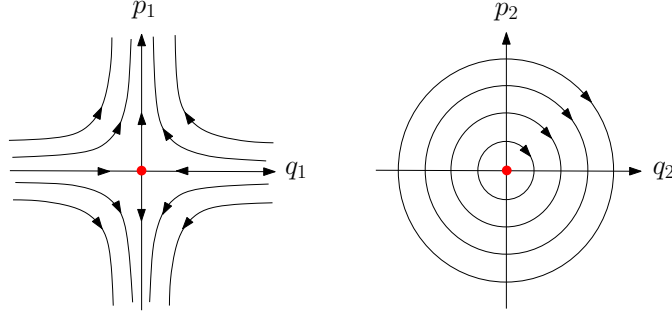


FIGURE 2.1. Local behavior of the flow near a saddle-center equilibrium point projected to the planes (q_1, p_1) and (q_2, p_2) , respectively.

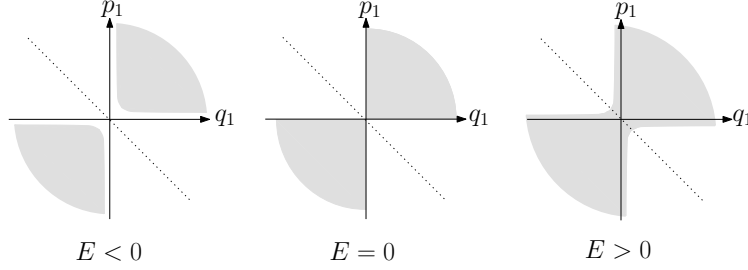


FIGURE 2.2. The projections of $K^{-1}(E)$ to the plane (q_1, p_1) for $E < 0$, $E = 0$ and $E > 0$, respectively.

Our first global assumption on the Hamiltonian function H is that $\varphi(N_0^\delta)$ is also the boundary of an embedded closed 3-ball $B_\delta \subset H^{-1}(0)$ which contains only regular points of H . We obtain what we call a sphere-like singular subset

$$S_0 := \varphi(B_0^\delta) \cup B_\delta \subset H^{-1}(0),$$

which is homeomorphic to a 3-sphere and contains only regular points of H , except for the saddle-center p_c as its unique singularity. See Figure 2.3.

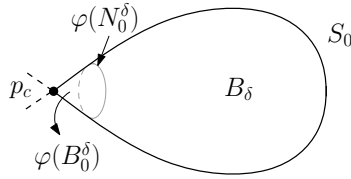


FIGURE 2.3. The sphere-like singular subset $S_0 = \varphi(B_0^\delta) \cup B_\delta \subset H^{-1}(0)$.

It follows from the assumptions on S_0 that, for all energies $E > 0$ sufficiently small, the energy level $H^{-1}(E)$ contains a subset S_E close to S_0 which is diffeomorphic to the closed 3-ball and whose boundary is given in local coordinates by

$$\varphi^{-1}(\partial S_E) = K^{-1}(E) \cap \{q_1 + p_1 = 0\}.$$

From now on we shall identify the points $U \simeq V$ under the change of coordinates φ in order to simplify the notation. Locally, the projection of S_E to the (q_1, p_1) -plane lies in $\{q_1 + p_1 \geq 0\}$. Notice that ∂S_E contains the periodic orbit

$$P_{2,E} := K^{-1}(E) \cap \{q_1 = p_1 = 0\},$$

called Lyapunoff orbit, which lies in the center manifold of p_c . See Figure 2.4. It is well known that $P_{2,E}$ is hyperbolic inside its energy level $H^{-1}(E)$ and its Conley-Zehnder index equals 2, see [8, Proposition 4.5].

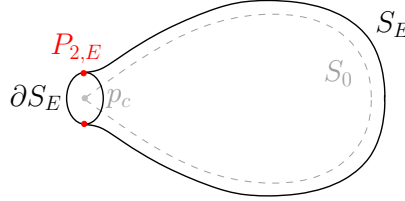


FIGURE 2.4. The embedded closed 3-ball $S_E \subset H^{-1}(E)$, $E > 0$ small.

Since $\partial_{I_2} \bar{K}(0, 0) = \omega \neq 0$, we can write

$$I_2 = I_2(I_1, E) = \frac{E}{\omega} + \frac{\alpha}{\omega} I_1 + O(I_1^2 + E^2),$$

for $|E|, |I_1|$ sufficiently small with $I_2(0, 0) = 0$. Thus the periodic orbit $P_{2,E}$ is given by

$$q_1 = p_1 = 0, \quad q_2^2 + p_2^2 = 2I_2(0, E) = 2\frac{E}{\omega} + O(E^2).$$

The Hamiltonian period of $P_{2,E}$ is given by

$$T_{2,E}^H = \frac{2\pi}{\bar{\omega}(0, I_2(0, E))},$$

where $\bar{\omega}(0, I_2(0, E)) = \partial_{I_2} \bar{K}(0, I_2(0, E)) = \omega + O(E)$.

We are interested in studying the Hamiltonian dynamics on the 3-ball $S_E \subset H^{-1}(E)$. Consider the hemispheres of ∂S_E given by

$$U_{1,E} = K^{-1}(E) \cap \{q_1 + p_1 = 0, q_1 < 0\},$$

$$U_{2,E} = K^{-1}(E) \cap \{q_1 + p_1 = 0, q_1 > 0\},$$

so that $\partial S_E = U_{1,E} \cup P_{2,E} \cup U_{2,E}$. See Figure 2.5.

The stable and unstable manifolds of $P_{2,E}$ are denoted by $W^s(P_{2,E})$ and $W^u(P_{2,E})$, respectively. Locally, such manifolds are given by

$$W_{\text{loc}}^s(P_{2,E}) := \{p_1 = 0, q_2^2 + p_2^2 = 2I_2(0, E)\},$$

$$W_{\text{loc}}^u(P_{2,E}) := \{q_1 = 0, q_2^2 + p_2^2 = 2I_2(0, E)\}.$$

Let us consider only the branches of $W_{\text{loc}}^s(P_{2,E})$ and $W_{\text{loc}}^u(P_{2,E})$ contained in $\dot{S}_E := S_E \setminus \partial S_E$.

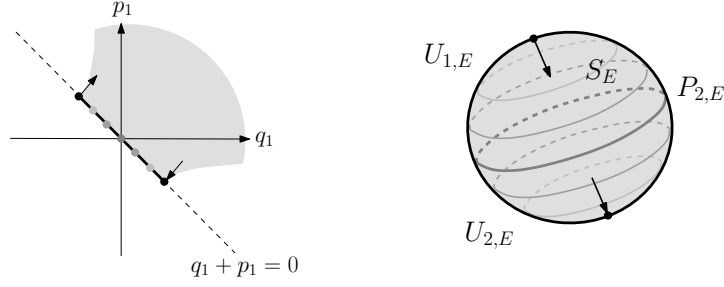


FIGURE 2.5. The embedded 2-sphere $\partial S_E = U_{1,E} \cup P_{2,E} \cup U_{2,E}$ and its projection to the plane (q_1, p_1) .

Definition 2.1. A 2 – 3 foliation of S_E adapted to the Hamiltonian flow is a singular foliation \mathcal{F}_E of $S_E \subset H^{-1}(E)$ so that:

- (i) The singular set of \mathcal{F}_E is formed by $P_{2,E} \subset \partial S_E$ and a periodic orbit $P_{3,E} \subset \dot{S}_E$, which is unknotted and has Conley-Zehnder index 3.
- (ii) \mathcal{F}_E contains the hemispheres $U_{1,E}$ and $U_{2,E}$ in ∂S_E as regular leaves. These leaves are called rigid planes.
- (iii) \mathcal{F}_E contains a cylinder V_E in \dot{S}_E whose closure has boundary $P_{3,E} \cup P_{2,E}$. V_E is called a rigid cylinder.
- (iv) \mathcal{F}_E contains a one parameter family of planes $D_{\tau,E}, \tau \in (0, 1)$, foliating $\dot{S}_E \setminus (P_{3,E} \cup V_E)$. The closure of each $D_{\tau,E}$ has boundary $P_{3,E}$. As $\tau \rightarrow 0^+$, $D_{\tau,E}$ C^0 -converges to $V_E \cup P_{2,E} \cup U_{1,E}$ and, as $\tau \rightarrow 1^-$, $D_{\tau,E}$ C^0 -converges to $V_E \cup P_{2,E} \cup U_{2,E}$.
- (v) All regular leaves $U_{1,E}, U_{2,E}, V_E$ and $D_{\tau,E}, \tau \in (0, 1)$, are transverse to the Hamiltonian vector field X_H .

See Figure 2.6.

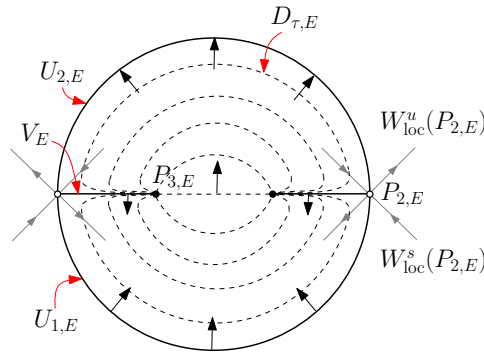


FIGURE 2.6. A section of a 2 – 3 foliation of S_E . The black arrows point to the same direction of the Hamiltonian vector field.

Definition 2.2. We say that the sphere-like subset $S_0 \subset H^{-1}(0)$ containing the saddle-center p_c is a strictly convex singular subset of $H^{-1}(0)$ if S_0 bounds a convex

subset of \mathbb{R}^4 and the Hessian of H restricted to $T\dot{S}_0$ is everywhere positive-definite. Here $\dot{S}_0 = S_0 \setminus \{p_c\}$.

It is proved in [8] that if S_0 is a strictly convex singular subset of $H^{-1}(0)$ then S_E admits a 2 – 3 foliation for all $E > 0$ sufficiently small.

Theorem 2.3. [8, Theorem 1.9 and Corollary 1.10] *Let $H : \mathbb{R}^4 \rightarrow \mathbb{R}$ be a smooth Hamiltonian function. Assume that H admits a saddle-center equilibrium point $p_c \in H^{-1}(0)$ so that, near p_c , H is real-analytic and takes the form (2.1) for suitable local real-analytic symplectic coordinates. Assume moreover that p_c lies in a strictly convex singular subset $S_0 \subset H^{-1}(0)$. Then, for all $E > 0$ sufficiently small, the embedded closed 3-ball $S_E \subset H^{-1}(E)$ near S_0 , defined as above, admits a 2 – 3 foliation adapted to the Hamiltonian flow. In particular, $P_{2,E}$ admits a homoclinic orbit inside $S_E \setminus \partial S_E$.*

The main result of this paper is the following theorem which asserts that if the Hamiltonian function in Theorem 2.3 is real-analytic then one obtains infinitely many periodic orbits and homoclinics to $P_{2,E}$ inside the closed 3-ball S_E .

Theorem 2.4. *Let $H : \mathbb{R}^4 \rightarrow \mathbb{R}$ be a real-analytic Hamiltonian function. Assume that H admits a saddle-center equilibrium point $p_c \in H^{-1}(0)$ so that H takes the form (2.1) for suitable local real-analytic symplectic coordinates near p_c . Assume moreover that p_c lies in a strictly convex singular subset $S_0 \subset H^{-1}(0)$. Let $S_E \subset H^{-1}(E)$, $E > 0$ small, be the topological closed 3-ball near S_0 , defined as above. Then for all $E > 0$ sufficiently small there exist infinitely many periodic orbits and infinitely many homoclinics to $P_{2,E}$ inside $S_E \setminus \partial S_E$. Moreover, if the branches of $W^s(P_{2,E})$ and $W^u(P_{2,E})$ contained in $S_E \setminus \partial S_E$ do not coincide then the Hamiltonian flow restricted to $H^{-1}(E)$ has positive topological entropy.*

3. APPLICATIONS

Hamiltonian functions admitting saddle-center equilibrium points are easily found in literature. For instance, if the Hamiltonian $H : \mathbb{R}^4 \rightarrow \mathbb{R}$ is written as kinetic plus potential energy

$$(3.1) \quad H(x, y, p_x, p_y) = \frac{p_x^2 + p_y^2}{2} + V(x, y),$$

then $(x_c, y_c) \in \mathbb{R}^2$ is a saddle-type critical point for V if and only if $p_c = (x_c, y_c, 0, 0) \in \mathbb{R}^4$ is a saddle-center equilibrium point for H .

In case H has the form (3.1), the convexity condition found in Theorems 2.3 and 2.4 can be checked in terms of the potential function V on the corresponding Hill's region.

Proposition 3.1 ([24], Theorem 1). *Let $H : \mathbb{R}^4 \rightarrow \mathbb{R}$ be a Hamiltonian function given as in (3.1), where $V : \mathbb{R}^2 \rightarrow \mathbb{R}$ is a smooth function. Let $S \subset H^{-1}(E_0)$ be a sphere-like singular subset of the level set $H^{-1}(E_0)$, with a singularity p_c corresponding to a saddle-center equilibrium point. Let $\pi : \mathbb{R}^4 \rightarrow \mathbb{R}^2$ be the projection $\pi(x, y, p_x, p_y) = (x, y)$ and let $B := \pi(S)$. Then S is a strictly convex singular subset of $H^{-1}(E_0)$ if and only if*

$$(3.2) \quad 2(E_0 - V)(V_{xx}V_{yy} - V_{xy}^2) + V_{xx}V_y^2 + V_{yy}V_x^2 - 2V_xV_yV_{xy} > 0$$

for all points in $\pi(S \setminus \{p_c\}) = B \setminus \{\pi(p_c)\}$. This statement also holds if S is diffeomorphic to the 3-sphere and inequality (3.2) holds at the disk-like region $B = \pi(S)$.

If the Hamiltonian $H : \mathbb{R}^4 \rightarrow \mathbb{R}$ has the form

$$(3.3) \quad H(x, y, p_x, p_y) = \frac{1}{2} [(p_x - A_1(x, y))^2 + (p_y - A_2(x, y))^2] + V(x, y),$$

where the magnetic vector potential $A = (A_1, A_2)$ is linear, then strict convexity of the singular subset does not depend on A and can be directly checked using inequality (3.2) on the corresponding Hill's region $\pi(S \setminus \{p_c\})$.

In the following sections we present some examples of Hamiltonians of the form kinetic plus potential energy for which our main results apply. In particular, such systems admit infinitely many periodic orbits and homoclinics to the Lyapunoff orbit near the critical energy level containing a saddle-center equilibrium. Motivated by the Allen-Cahn equation, Fusco-Gronchi-Novaga [12, 13] use variational methods to study the existence of periodic motions of kinetic plus potential Hamiltonians.

3.1. Buckled nanobeams. The transverse displacement of a nanobeam subjected to a longitudinal compressive stress applied at both ends is studied in [4, 5]. Under a certain compression, the linearized dynamics over the equilibrium state can be formulated in terms of a two-degree-of-freedom Hamiltonian system, which is obtained by a two-mode Galerkin truncation of the infinite dimensional dynamics described by the Euler-Bernoulli beam equation. The Hamiltonian function describing such a truncated dynamics is given by

$$(3.4) \quad H(x, y, p_x, p_y) = \frac{p_x^2 + p_y^2}{2} + V(x, y),$$

where the potential function V has the form

$$(3.5) \quad V(x, y) = \alpha x^2 + 4\beta y^2 + \frac{1}{2} (x^2 + 4y^2)^2$$

with real parameters $\alpha < 0$ and $\beta \neq 0$. Notice that V is symmetric with respect to x and y .

Let us assume that $\beta > 0$. In this case, H admits a saddle-center equilibrium at $p_c := (0, 0, 0, 0) \in H^{-1}(0)$ corresponding to a saddle of the potential function V . The critical energy level $H^{-1}(0)$ contains a pair of singular subsets S and S' , both homeomorphic to S^3 , intersecting at the common singularity p_c . Their projections B and B' to the plane (x, y) , respectively, are depicted in Figure 3.1.

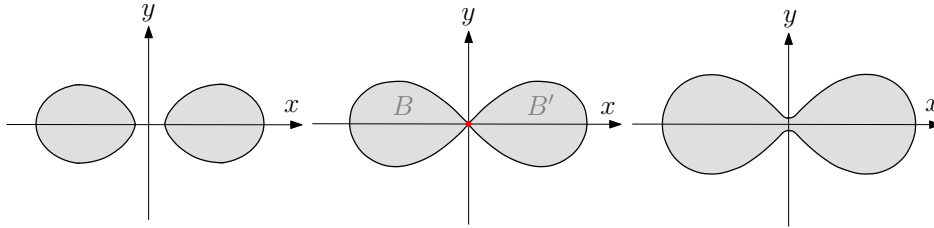


FIGURE 3.1. Hill's regions of the Hamiltonian function defined by (3.4) and (3.5) for energies $E < 0$, $E = 0$ and $E > 0$, respectively, for $|E|$ small. S and S' project to B and B' , respectively.

Proposition 3.2. *Assume that $\alpha < 0 < \beta$. Then the sphere-like singular subsets S and S' are strictly convex.*

Proof. Consider the disks $B = \pi(S)$ and $B' = \pi(S')$, where $\pi : \mathbb{R}^4 \rightarrow \mathbb{R}^2$ is the canonical projection $\pi(x, y, p_x, p_y) = (x, y)$. From (3.4) we see that $V \leq 0$ for all points in $B \cup B' \subset \pi(H^{-1}(0))$, i.e.,

$$(3.6) \quad \alpha x^2 + 4\beta y^2 + \frac{1}{2}(x^2 + 4y^2)^2 \leq 0, \quad \forall (x, y) \in B \cup B'.$$

According to Proposition 3.1, a necessary and sufficient condition for S and S' to be strictly convex singular subsets is that

$$(3.7) \quad T := -2V \det \text{Hess} V + V_{xx}V_y^2 + V_{yy}V_x^2 - 2V_xV_yV_{xy} > 0$$

for all points in $D := B \cup B' \setminus \{(0, 0)\}$. A straightforward computation shows that

$$T = -16(x^2 + 4y^2)^2 \left[(x^2 + 4y^2)^2 + \alpha(3\beta + 3x^2 + 4y^2) + \beta(x^2 + 12y^2) \right],$$

and hence we just need to prove that

$$C := (x^2 + 4y^2)^2 + \alpha(3\beta + 3x^2 + 4y^2) + \beta(x^2 + 12y^2) < 0$$

for all $(x, y) \in D$.

Using (3.6) one can check that

$$(3.8) \quad C \leq 3\alpha\beta + (\alpha + \beta)(x^2 + 4y^2)$$

in D . If $\alpha + \beta \leq 0$ then inequality (3.8) directly implies that $C < 0$ in D since $\alpha < 0 < \beta$. Let us assume that $\alpha + \beta > 0$. In this case,

$$3\alpha\beta + (\alpha + \beta)(x^2 + 4y^2) < 0 \Leftrightarrow x^2 + 4y^2 < -\frac{3\alpha\beta}{\alpha + \beta}$$

and therefore, in order to prove that the function $C = C(x, y)$ is negative on D , we need to check that D is contained in the open subset bounded by the ellipse

$$x^2 + 4y^2 = -\frac{3\alpha\beta}{\alpha + \beta}.$$

It is sufficient to show this condition for points in the boundary ∂D .

Let $U : \mathbb{R}^2 \rightarrow \mathbb{R}$ be given by $U(x, y) := x^2 + 4y^2$. Equality in (3.6) holds if and only if $(x, y) \in \partial D$. This means that

$$(3.9) \quad U^2 + 2\alpha U + 8(\beta - \alpha)y^2 = 0$$

for all points in ∂D . The solutions of the polynomial (3.9) in U are given by

$$U = \frac{-2\alpha \pm \sqrt{4\alpha^2 - 32(\beta - \alpha)y^2}}{2}.$$

Thus, the maximum value of U on the boundary ∂D is assumed when $y = 0$, for which $U = -2\alpha > 0$ and $x = \pm\sqrt{-2\alpha}$. Using again that $\alpha + \beta > 0$, we see that $U(\pm\sqrt{-2\alpha}, 0) = -2\alpha < -\frac{3\alpha\beta}{\alpha + \beta}$ is equivalent to $2\alpha^2 > \alpha\beta$, which clearly holds since $\alpha < 0 < \beta$. This proves that

$$(3.10) \quad U(x, y) < -\frac{3\alpha\beta}{\alpha + \beta}, \quad \forall (x, y) \in \partial D,$$

as desired, and hence $C < 0$ on D in case $\alpha + \beta > 0$ as well.

We conclude that $T = T(x, y)$, given by (3.7), is positive on D . Theorem 3.1 implies that the subsets $S, S' \subset H^{-1}(0)$ containing the saddle-center $p_c = (0, 0, 0, 0)$ are both strictly convex. \square

For all $E > 0$ sufficiently small, the energy level $H^{-1}(E)$ contains closed 3-balls S_E and S'_E near S and S' , respectively, so that $\partial S_E = \partial S'_E$ and $W_E := S_E \cup S'_E$ is an embedded 3-sphere. The projection of $W_E \subset H^{-1}(E)$ to the plane (x, y) is represented in the right-most drawing in Figure 3.1.

It follows from Proposition 3.2 and Theorem 2.3 that both S_E and S'_E admit $2-3$ foliations, denoted by \mathcal{F}_E and \mathcal{F}'_E , respectively, such that the Lyapunoff orbit $P_{2,E} \subset \partial S_E = \partial S'_E$ is a binding orbit for both \mathcal{F}_E and \mathcal{F}'_E . In this case, the singular foliation $\mathcal{F}_E \cup \mathcal{F}'_E$ is what we call a $3-2-3$ foliation adapted to Hamiltonian flow on W_E , see Figure 3.2 and [8, Remark 1.11]. Theorem 2.4 ensures the existence of infinitely many periodic orbits and infinitely many homoclinics to $P_{2,E}$ in each subset $S_E \setminus \partial S_E$ and $S'_E \setminus \partial S'_E$.

Theorem 3.3. *For all $E > 0$ sufficiently small, W_E admits a $3-2-3$ foliation. In particular, W_E contains infinitely many periodic orbits and infinitely many homoclinics to the Lyapunoff orbit $P_{2,E}$ in the center manifold of the saddle-center $0 \in \mathbb{R}^4$.*

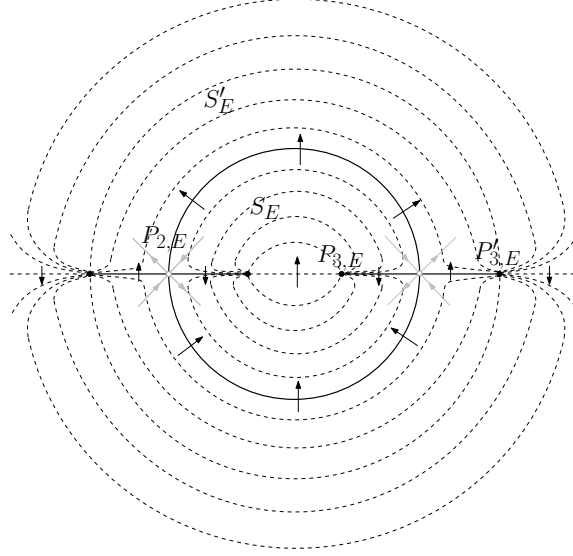


FIGURE 3.2. A section of a $3-2-3$ foliation on $W_E = S_E \cup S'_E$. The black arrows point to the same direction of the Hamiltonian vector field.

3.2. The Hénon-Heiles Hamiltonian. Let $H : \mathbb{R}^4 \rightarrow \mathbb{R}$ be the Hamiltonian defined by

$$(3.11) \quad H(x, y, p_x, p_y) = \frac{p_x^2 + p_y^2}{2} + \frac{x^2 + y^2}{2} + bx^2y - \frac{y^3}{3}$$

which depends on a parameter $0 < b < 1$. The case $b = 1$ is known as Hénon-Heiles Hamiltonian and it models the motion of stars around a galactic center.

The Hamiltonian H admits a saddle-center equilibrium at $p_c = (0, 1, 0, 0) \in H^{-1}(\frac{1}{6})$. Moreover, for all $0 < b < 1$, p_c lies in a strictly convex singular subset $S_0 \subset H^{-1}(\frac{1}{6})$, see [24] for a proof. The projection B of S_0 to the (x, y) -plane is seen in Figure 3.3.

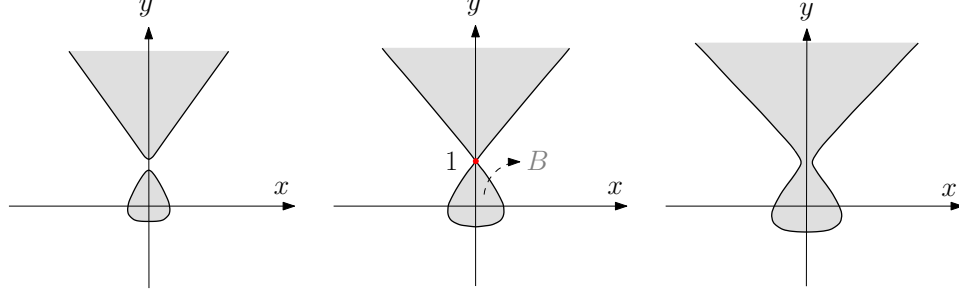


FIGURE 3.3. Hill's regions of the Hamiltonian function (3.11) for energies $E < \frac{1}{6}$, $E = \frac{1}{6}$ and $E > \frac{1}{6}$ respectively, with $|E - \frac{1}{6}|$ small.

As observed in [8, §1.5], Theorem 2.3 gives a $2 - 3$ foliation \mathcal{F}_E defined on an embedded closed 3-ball $S_E \subset H^{-1}(E)$ near S_0 for each $E > \frac{1}{6}$ sufficiently close to $\frac{1}{6}$. One of the binding orbits of \mathcal{F}_E is the Lyapunoff orbit $P_{2,E} \subset \partial S_E$. Theorem 2.4 implies the following result.

Theorem 3.4. *For every $E > \frac{1}{6}$ sufficiently close to $\frac{1}{6}$ the Hamiltonian flow on the closed 3-ball $S_E \subset H^{-1}(E)$ admits infinitely many periodic orbits and infinitely many homoclinics to the Lyapunoff orbit $P_{2,E}$. Moreover, if the branches of the stable and unstable manifolds of $P_{2,E}$ inside S_E do not coincide then the topological entropy of the Hamiltonian flow restricted to $H^{-1}(E)$ is positive.*

3.3. Charged particles in planetary magnetospheres. The motion of a dust particle in a planetary magnetosphere, whose dynamics is dominated by gravitational and eletromagnetic forces, is studied in [14], see also [7, 17, 19, 26]. Under some strong simplifying assumptions, this problem can be reduced to a two-degree-of-freedom Hamiltonian system in \mathbb{R}^4 with Hamiltonian function given by

$$(3.12) \quad H(x, z, p_x, p_z) = \frac{p_x^2 + p_z^2}{2} + V(x, z),$$

where V is the potential function

$$(3.13) \quad V(x, z) = -\epsilon x + \frac{a^2}{3}x^3 + \frac{c^2}{2}z^2$$

depending on the parameters $a, c, \epsilon > 0$.

The points

$$p_1 = \left(-\frac{\sqrt{\epsilon}}{a}, 0\right) \quad \text{and} \quad p_2 = \left(\frac{\sqrt{\epsilon}}{a}, 0\right)$$

are critical points of V and hence $P_1 := (p_1, 0, 0)$ and $P_2 := (p_2, 0, 0)$ are equilibrium points of the Hamiltonian flow of H . Their energies are given by

$$(3.14) \quad E_1 = H(P_1) = \frac{2\epsilon\sqrt{\epsilon}}{3a} \quad \text{and} \quad E_2 = H(P_2) = -\frac{2\epsilon\sqrt{\epsilon}}{3a}.$$

Since $\text{Hess}V(x, z) = \text{Diag}(2a^2x, c^2)$ we see that P_1 is a saddle-center equilibrium point of H and P_2 corresponds to a local minimum. We shall prove that for any $a, c, \epsilon > 0$ the saddle-center P_1 lies in a strictly convex singular subset $S_0 \subset H^{-1}(E_1)$.

Let $\pi : \mathbb{R}^4 \rightarrow \mathbb{R}^2$ be the canonical projection

$$(3.15) \quad \pi(x, z, p_x, p_z) = (x, z).$$

The projection $\pi(H^{-1}(E_1))$ has a subset B homeomorphic to the closed disk which contains $\pi(P_1) = p_1$. The boundary ∂B is a closed curve in \mathbb{R}^2 , which is regular except at p_1 , and its points satisfy $V = E_1$. See Figure 3.4. Since $V(-\sqrt{\epsilon}/a, 0) = V(2\sqrt{\epsilon}/a, 0) = E_1$ we see from (3.13) that

$$(3.16) \quad B \subset \left\{ (x, z) \in \mathbb{R}^2 \mid -\frac{\sqrt{\epsilon}}{a} \leq x \leq 2\frac{\sqrt{\epsilon}}{a} \right\}.$$

The subset $S_0 := \pi^{-1}(B) \cap H^{-1}(E_1)$ contains the saddle-center P_1 , is homeomorphic to the 3-sphere S^3 and $\dot{S}_0 := S_0 \setminus \{P_1\}$ is a regular hypersurface of \mathbb{R}^4 .

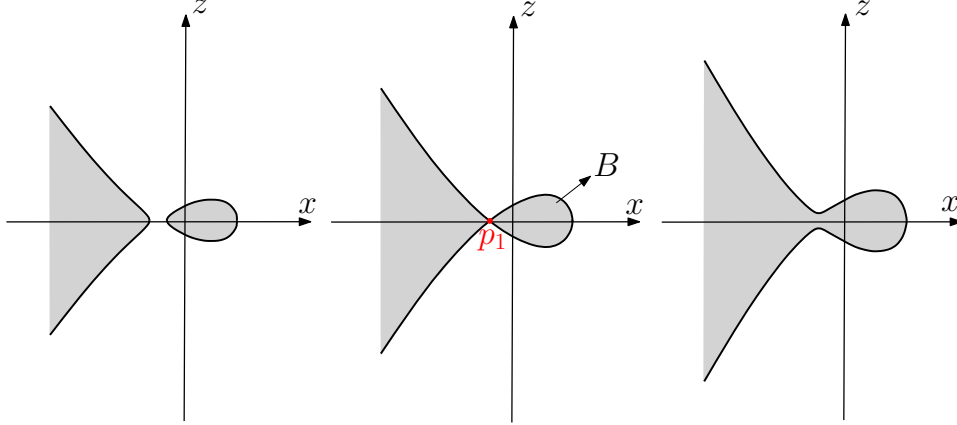


FIGURE 3.4. Hill's regions of the Hamiltonian function (3.12) for energies $E < E_1$, $E = E_1$ and $E > E_1$ respectively, with $|E - E_1|$ small.

Proposition 3.5. *For all $a, c, \epsilon > 0$, the sphere-like singular subset $S_0 = \pi^{-1}(B) \cap H^{-1}(E_1)$ is strictly convex.*

Proof. In order to prove that S_0 is strictly convex we need to verify the condition

$$M := 2(E_1 - V) \det \text{Hess}V + V_{xx}V_z^2 + V_{zz}V_x^2 - 2V_xV_zV_{xz} > 0,$$

for all points in $\dot{B} := B \setminus \{p_1\}$, see Proposition 3.1. A direct computation shows that

$$M(x, z) = \frac{c^2}{3}g(x),$$

where

$$g(x) = -a^4x^4 + 6a^2\epsilon x^2 + 8a\epsilon\sqrt{\epsilon}x + 3\epsilon^2.$$

So it is sufficient to check that $g(x) > 0$ for all $x \in \left(-\frac{\sqrt{\epsilon}}{a}, 2\frac{\sqrt{\epsilon}}{a}\right]$.

Defining $u := \frac{a}{\sqrt{\epsilon}}x$, we reduce to proving that $q(u) > 0$ on $(-1, 2]$, where

$$q(u) = -u^4 + 6u^2 + 8u + 3.$$

One can easily see that $u = -1$ and $u = 3$ are roots of q with multiplicities 3 and 1, respectively, and thus q is positive on $(-1, 2]$. Consequently, M is positive on \dot{B} . We conclude from Theorem 3.1 that $S_0 \subset H^{-1}(E_1)$ is a strictly convex singular subset of $H^{-1}(E_1)$ which contains the saddle-center P_1 . \square

Proposition 3.5 together with Theorems 2.3 and 2.4 imply the following theorem.

Theorem 3.6. *Fix $\epsilon, a, c > 0$ and let E_1 be as in (3.14). For every $E - E_1 > 0$ sufficiently small the closed 3-ball $S_E \subset H^{-1}(E)$ admits a 2 – 3 foliation adapted to the Hamiltonian flow. Moreover, S_E admits infinitely many periodic orbits and infinitely many homoclinics to $P_{2,E}$. Since H is integrable, the branches of the stable and unstable manifolds of $P_{2,E}$ inside S_E coincide.*

4. EXISTENCE OF A HOMOCLINIC TO THE LYAPUNOFF ORBIT

Consider the 2 – 3 foliation \mathcal{F}_E on the 3-ball $S_E \subset H^{-1}(E)$ as the one obtained in Theorem 2.3, for $E > 0$ small. The foliation \mathcal{F}_E contains a one parameter family of planes $D_{\tau,E}$, $\tau \in (0, 1)$, each one transverse to the Hamiltonian vector field X_H , so that the closure of $D_{\tau,E}$ has the periodic orbit $P_{3,E}$ as boundary. We shall study the first return map to such leaves, where it is defined, in order to prove multiplicity of periodic orbits and homoclinics to $P_{2,E}$ in $\dot{S}_E = S_E \setminus \partial S_E$. In the following we fix $E > 0$ small and assume the existence of the 2 – 3 foliation \mathcal{F}_E on $S_E \subset H^{-1}(E)$. From now on we may omit the dependence on E in the notation for simplicity.

For all $0 < \tau_0 < 1$ sufficiently close to 0, the branch $W_{\text{loc}}^u(P_{2,E})$ of the local unstable manifold of $P_{2,E}$ inside \dot{S}_E intersects the plane D_{τ_0} on an embedded circle $C_{\tau_0}^u$. All points in the interior of the closed disk $B_{\tau_0}^u \subset D_{\tau_0}$ bounded by $C_{\tau_0}^u$ correspond to trajectories just entering S_E through the hemisphere $U_{1,E}$. Similarly, for $0 < \tau_1 < 1$ sufficiently close to 1, the branch of the local stable manifold $W_{\text{loc}}^s(P_{2,E})$ inside \dot{S}_E intersects D_{τ_1} on an embedded circle denoted by $C_{\tau_1}^s$. All points in the interior of the closed disk $B_{\tau_1}^s \subset D_{\tau_1}$ bounded by $C_{\tau_1}^s$ correspond to trajectories which exit S_E through the hemisphere $U_{2,E}$.

Due to the existence of the 2 – 3 foliation on S_E , the Hamiltonian flow induces the following symplectomorphisms:

- A global transition map

$$(4.1) \quad \Psi^g : D_{\tau_0} \rightarrow D_{\tau_1}$$

defined as follows: if $x \in D_{\tau_0}$, then $\Psi^g(x)$ is the first point in the positive trajectory through x which hits D_{τ_1} . Such diffeomorphism preserves the canonical symplectic form restricted to the disks D_{τ_0} and D_{τ_1} .

- A local transition map

$$(4.2) \quad \Psi^l : D_{\tau_1} \setminus B_{\tau_1}^s \rightarrow D_{\tau_0} \setminus B_{\tau_0}^u$$

defined as follows: if $x \in D_{\tau_1} \setminus B_{\tau_1}^s$, then $\Psi^l(x)$ is the first point in the positive trajectory through x which hits the annulus $D_{\tau_0} \setminus B_{\tau_0}^u$. Such diffeomorphism preserves the canonical symplectic form restricted to the annuli $D_{\tau_1} \setminus B_{\tau_1}^s$ and $D_{\tau_0} \setminus B_{\tau_0}^u$. Later on we shall use Moser's coordinates to describe Ψ^l near the boundary component $C_{\tau_1}^s$.

The existence of the global and local maps above follows from the fact that the Conley-Zehnder index of $P_{3,E}$ is 3 and by a precise description of the asymptotic behavior of the regular leaves D_τ , $0 < \tau < 1$, close to $P_{3,E}$. See [8] and [15].

Using these transition maps we can prove that the 2 – 3 foliation in S_E forces the existence of at least one homoclinic orbit to $P_{2,E}$ contained in \dot{S}_E .

Proposition 4.1. *The open 3-ball \dot{S}_E contains at least one homoclinic orbit to $P_{2,E}$.*

Proposition 4.1 follows directly from Proposition 4.2 below. It relies on standard arguments based on preservation of area, see [1] and [16]. We include it here for completeness.

Proposition 4.2. *Let Ψ^g and Ψ^l be the global and local symplectomorphisms defined in (4.1) and (4.2), respectively. Let $C_{\tau_0}^u$ and $C_{\tau_1}^s$ be the intersections of $W_{\text{loc}}^u(P_{2,E})$ and $W_{\text{loc}}^s(P_{2,E})$ with D_{τ_0} and D_{τ_1} respectively. Then there exists $N \in \mathbb{N}^*$ so that $(\Psi^g \circ \Psi^l)^{N-1} \circ \Psi^g|_{C_{\tau_0}^u}$ is well-defined and*

$$(\Psi^g \circ \Psi^l)^{N-1} \circ \Psi^g(C_{\tau_0}^u) \cap C_{\tau_1}^s \neq \emptyset.$$

Proof. If $\Psi^g(C_{\tau_0}^u) \cap C_{\tau_1}^s \neq \emptyset$ then $N = 1$ and the proof is finished. Otherwise $\Psi^g(C_{\tau_0}^u)$ bounds a closed disk $B_1^u := \Psi^g(B_{\tau_0}^u)$ which is necessarily contained in $D_{\tau_1} \setminus B_{\tau_1}^s$. This follows from the fact that Ψ^g preserves an area form and both disks $B_{\tau_0}^u$ and $B_{\tau_1}^s$ have the same area $T_{2,E}$. In this case $\Psi^g \circ \Psi^l|_{B_1^u}$ is well-defined and we define $B_2^u := \Psi^g \circ \Psi^l(B_1^u)$. If $\partial B_2^u \cap C_{\tau_1}^s \neq \emptyset$, then $N = 2$ and the proof is finished. Otherwise, the closed disk B_2^u , which also has symplectic area $T_{2,E}$, is contained in $D_{\tau_1} \setminus B_{\tau_1}^s$ and must be disjoint from B_1^u (note that $\Psi^l(B_1^u)$ is contained in $D_{\tau_0} \setminus B_{\tau_0}^u$). In this case $\Psi^g \circ \Psi^l|_{B_2^u}$ is well-defined and we define $B_3^u := \Psi^g \circ \Psi^l(B_2^u)$. Arguing inductively, if $\partial B_j^u \cap C_{\tau_1}^s \neq \emptyset$, then $N = j$ and the proof is finished. Otherwise, the closed disk B_j^u , which also has symplectic area $T_{2,E}$, is contained in $D_{\tau_1} \setminus (B_{\tau_1}^s \cup (\cup_{1 \leq k < j} B_k^u))$. In this case $\Psi^g \circ \Psi^l|_{B_j^u}$ is well-defined and we define $B_{j+1}^u := \Psi^g \circ \Psi^l(B_j^u)$. Since the symplectic area of $D_{\tau_1} \setminus B_{\tau_1}^s$ is finite and all B_j^u are disjoint and have the same symplectic area $T_{2,E} > 0$, this process has to terminate after finitely many steps, i.e., there exists $N \in \mathbb{N}$ so that $\Psi^g \circ \Psi^l|_{B_{N-1}^u}$ is well-defined and $B_N^u := \Psi^g \circ \Psi^l(B_{N-1}^u)$ intersects $B_{\tau_1}^s$. In particular, $(\Psi^g \circ \Psi^l)^{N-1} \circ \Psi^g|_{C_{\tau_0}^u}$ is well-defined and $(\Psi^g \circ \Psi^l)^{N-1} \circ \Psi^g(C_{\tau_0}^u) \cap C_{\tau_1}^s \neq \emptyset$, finishing the proof of the proposition. \square

Let $N \in \mathbb{N}$ be as in Proposition 4.2. From now on we use the notations

$$\begin{aligned} B_N^u &:= (\Psi^g \circ \Psi^l)^{N-1} \circ \Psi^g(B_{\tau_0}^u) \subset D_{\tau_1} \\ C_N^u &:= \partial B_N^u = (\Psi^g \circ \Psi^l)^{N-1} \circ \Psi^g(C_{\tau_0}^u) \subset D_{\tau_1}. \end{aligned}$$

We know that $C_N^u \cap C_{\tau_1}^s \neq \emptyset$ and we consider two distinct situations: either $C_N^u \neq C_{\tau_1}^s$ or $C_N^u = C_{\tau_1}^s$.

In the first case where $C_N^u \neq C_{\tau_1}^s$, we shall prove that the Hamiltonian flow on \dot{S}_E admits infinitely many transverse homoclinic orbits to $P_{2,E}$ and such transversality implies positivity of the topological entropy. In particular, we obtain infinitely many periodic orbits in \dot{S}_E . This is discussed in Section 6.

In the second case where $C_N^u = C_{\tau_1}^s$, we immediately obtain infinitely many homoclinic orbits to $P_{2,E}$ in \dot{S}_E . Moreover, the Hamiltonian flow defines a symplectomorphism $\Psi^N : \mathcal{A} \rightarrow \mathcal{A}$, where $\Psi := \Psi^g \circ \Psi^l$ and \mathcal{A} consists of D_{τ_1} with finitely many disjoint closed disks removed

$$\mathcal{A} := D_{\tau_1} \setminus \bigcup_{j=0}^{N-1} \Psi^{-j}(B_{\tau_1}^s).$$

Such map describes the dynamics on an invariant open subset $\mathcal{U}_{\mathcal{A}} \subset \dot{S}_E$ given by the trajectories in \dot{S}_E intersecting \mathcal{A} . Moreover, Ψ has an infinite twist near the inner boundary components of \mathcal{A} . Using results on area preserving homeomorphisms of the open annulus due to J. Franks, we shall derive infinitely many periodic points of Ψ , which correspond to infinitely many periodic orbits in \dot{S}_E . This is proved in Section 7.

5. INFINITE TWIST OF THE LOCAL TRANSITION MAP

In this section we construct local models for neighborhoods of $C_{\tau_1}^s \subset D_{\tau_1}$ and $C_{\tau_0}^u \subset D_{\tau_0}$, for a fixed $E > 0$ sufficiently small. We find suitable coordinates in order to describe the infinite twist of the local transition map Ψ^l near $C_{\tau_1}^s$.

Take $\delta > 0$ small. Consider the real-analytic open annuli $R_\delta^s, R_\delta^u \subset K^{-1}(E)$ given in Moser's coordinates (q_1, q_2, p_1, p_2) by

$$(5.1) \quad \begin{aligned} R_\delta^s &:= \left\{ (q_1, q_2, p_1, p_2) : q_1 = \delta, -\frac{\delta}{2} < p_1 < \frac{\delta}{2} \right\} \cap K^{-1}(E), \\ R_\delta^u &:= \left\{ (q_1, q_2, p_1, p_2) : p_1 = \delta, -\frac{\delta}{2} < q_1 < \frac{\delta}{2} \right\} \cap K^{-1}(E), \end{aligned}$$

and let $A_\delta^s \subset R_\delta^s$ and $A_\delta^u \subset R_\delta^u$ be defined by

$$(5.2) \quad \begin{aligned} A_\delta^s &:= \left\{ (q_1, q_2, p_1, p_2) : q_1 = \delta, 0 < p_1 < \frac{\delta}{2} \right\} \cap K^{-1}(E), \\ A_\delta^u &:= \left\{ (q_1, q_2, p_1, p_2) : p_1 = \delta, 0 < q_1 < \frac{\delta}{2} \right\} \cap K^{-1}(E). \end{aligned}$$

See Figure 5.1. Both R_δ^s and R_δ^u are transverse to the Hamiltonian vector field X_K . Observe that A_δ^s and A_δ^u correspond to non-transit trajectories of the Hamiltonian flow, i.e., those which do not cross the separating 2-sphere $\{q_1 + p_1 = 0\} \cap K^{-1}(E)$. In fact, A_δ^s is mapped onto A_δ^u by the local Hamiltonian flow.

Since $\partial_{I_1} \bar{K}(0, 0) = -\alpha \neq 0$, it follows from the implicit function theorem that there exists a real-analytic function f defined in a neighborhood of $(0, 0) \in \mathbb{R}^2$ such that

$$(5.3) \quad I_1 = f(I_2, E) = \frac{\omega}{\alpha} I_2 - \frac{E}{\alpha} + O(I_2^2 + E^2) \text{ with } \bar{K}(f(I_2, E), I_2) = E.$$

For the sake of simplicity we omit the dependence of f on E since $E > 0$ small is fixed.

Let $0 < I_2^\sharp < I_2^c < I_2^*$ be so that

$$f(I_2^\sharp) = -\frac{\delta^2}{2}, f(I_2^c) = 0 \text{ e } f(I_2^*) = \frac{\delta^2}{2}.$$

Taking $\delta > 0$ sufficiently small, we see that the local stable manifold $W_{\text{loc}}^s(P_{2,E})$ intersects the annulus R_δ^s along the real-analytic circle

$$(5.4) \quad S_\delta^s := \{q_1 = \delta, p_1 = 0, q_2^2 + p_2^2 = 2I_2^c\}$$

and the local unstable manifold $W_{\text{loc}}^u(P_{2,E})$ intersects the annulus R_δ^u on the real-analytic circle

$$(5.5) \quad S_\delta^u := \{q_1 = 0, p_1 = \delta, q_2^2 + p_2^2 = 2I_2^c\}.$$

See Figure 5.1.

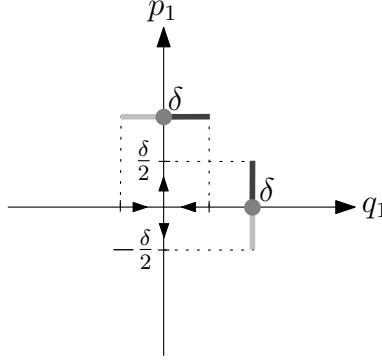


FIGURE 5.1. The transverse sections R_δ^s and R_δ^u , defined in (5.1), projected to the plane (q_1, p_1) . Each dark gray line represents the projection of one of the annuli A_δ^s and A_δ^u , defined in (5.2), and each gray dot represents the projection of one of the circles S_δ^s and S_δ^u , given in (5.4) and (5.5), respectively.

From now on it will be convenient to consider angle-action coordinates (θ, I_2) instead of the coordinates (q_2, p_2) , which are defined by the following relations:

$$q_2 = \sqrt{2I_2} \cos \theta \text{ and } p_2 = \sqrt{2I_2} \sin \theta.$$

In such coordinates, the circles S_δ^s and S_δ^u correspond to

$$(5.6) \quad S_c := \{(\theta, I_2) \in (\mathbb{R}/2\pi\mathbb{Z}) \times \mathbb{R}^+ : I_2 = I_2^c\},$$

the open annuli A_δ^s and A_δ^u correspond to

$$(5.7) \quad A_c^* := \{(\theta, I_2) \in (\mathbb{R}/2\pi\mathbb{Z}) \times \mathbb{R}^+ : I_2^c < I_2 < I_2^*\}$$

and the open annuli R_δ^s and R_δ^u correspond to

$$(5.8) \quad A_\sharp^* := \{(\theta, I_2) \in (\mathbb{R}/2\pi\mathbb{Z}) \times \mathbb{R}^+ : I_2^\sharp < I_2 < I_2^*\}.$$

We introduce the following real-analytic symplectic charts

$$(5.9) \quad \varphi_\delta^s : A_\sharp^* \rightarrow R_\delta^s \text{ and } \varphi_\delta^u : A_\sharp^* \rightarrow R_\delta^u$$

given by

$$(5.10) \quad \begin{aligned} \varphi_\delta^s(\theta, I_2) &= \left(\delta, \sqrt{2I_2} \cos \theta, \frac{f(I_2)}{\delta}, \sqrt{2I_2} \sin \theta \right), \\ \varphi_\delta^u(\theta, I_2) &= \left(\frac{f(I_2)}{\delta}, \sqrt{2I_2} \cos \theta, \delta, \sqrt{2I_2} \sin \theta \right), \end{aligned}$$

which satisfy $\varphi_\delta^s(S_c) = S_\delta^s$, $\varphi_\delta^s(A_c^*) = A_\delta^s$, $\varphi_\delta^u(S_c) = S_\delta^u$ and $\varphi_\delta^u(A_c^*) = A_\delta^u$. As a result, we obtain the real-analytic local model $(A_\#^*, A_c^*, S_c)$ for both $(R_\delta^s, A_\delta^s, S_\delta^s)$ and $(R_\delta^u, A_\delta^u, S_\delta^u)$. Notice that $(\varphi_\delta^u)^* \omega_0 = (\varphi_\delta^s)^* \omega_0 = d\theta \wedge dI_2$, where $\omega_0 = dp_1 \wedge dq_1 + dp_2 \wedge dq_2$.

Since $R_\delta^u, R_\delta^s, D_{\tau_0}$ and D_{τ_1} are transverse to the Hamiltonian vector field, one may use the positive Hamiltonian flow to obtain symplectomorphisms

$$(5.11) \quad \psi_{\tau_1, \delta}^s : V_{\tau_1}^s \rightarrow R_\delta^s \text{ and } \psi_{\delta, \tau_0}^u : R_\delta^u \rightarrow V_{\tau_0}^u$$

for $\delta > 0$ sufficiently small, where $V_{\tau_1}^s \subset D_{\tau_1}$ and $V_{\tau_0}^u \subset D_{\tau_0}$ are suitable annular neighborhoods of the circles $C_{\tau_1}^s \subset D_{\tau_1}$ and $C_{\tau_0}^u \subset D_{\tau_0}$, respectively, such that $\psi_{\tau_1, \delta}^s(C_{\tau_1}^s) = S_\delta^s$ and $\psi_{\delta, \tau_0}^u(S_\delta^u) = C_{\tau_0}^u$. Denoting

$$(5.12) \quad N_{\tau_1}^s := V_{\tau_1}^s \setminus B_{\tau_1}^s \text{ and } N_{\tau_0}^u := V_{\tau_0}^u \setminus B_{\tau_0}^u,$$

we observe that $\psi_{\tau_1, \delta}^s(N_{\tau_1}^s) = A_\delta^s$ and $\psi_{\delta, \tau_0}^u(A_\delta^u) = N_{\tau_0}^u$.

Using the maps defined in (5.9) and (5.11), we can consider from now on the angle-action coordinates $(\theta, I_2) \in A_\#^*$ on both annular neighborhoods $V_{\tau_1}^s \subset D_{\tau_1}$ and $V_{\tau_0}^u \subset D_{\tau_0}$, in such a way that $\psi_{\tau_1, \delta}^s$ and ψ_{δ, τ_0}^u correspond to the identity maps in coordinates (θ, I_2) . All this construction provides a local model $(A_\#^*, A_c^*, S_c)$ for both $(V_{\tau_1}^s, N_{\tau_1}^s, C_{\tau_1}^s)$ and $(V_{\tau_0}^u, N_{\tau_0}^u, C_{\tau_0}^u)$. The importance of this local model is that the transition maps induced by the Hamiltonian flow are real-analytic.

Now we give a description of the local transition map $\Psi^l : D_{\tau_1} \setminus B_{\tau_1}^s \rightarrow D_{\tau_0} \setminus B_{\tau_0}^u$, defined in (4.2), near the inner boundary circles $C_{\tau_1}^s = \partial B_{\tau_1}^s$ and $C_{\tau_0}^u = \partial B_{\tau_0}^u$, making use of the angle-action coordinates $(\theta, I_2) \in A_c^*$ on both $N_{\tau_1}^s \subset D_{\tau_1}$ and $N_{\tau_0}^u \subset D_{\tau_0}$.

By observing the behavior of the flow in local coordinates (q_1, q_2, p_1, p_2) , see Figure 2.1, we notice that positive trajectories starting at A_δ^s must hit A_δ^u . Since these solutions satisfy (2.2), one can compute the time that an orbit starting at A_δ^s takes to reach A_δ^u . This is given in angle-action coordinates by

$$T(\theta, I_2) = t(I_2) := -\frac{1}{\bar{\alpha}(I_2)} \ln \frac{f(I_2)}{\delta^2},$$

where

$$(5.13) \quad \bar{\alpha}(I_2) = \alpha - \partial_{I_1} R(f(I_2), I_2).$$

Note that $f(I_2)$ is positive on A_c^* and, as $I_2 \rightarrow (I_2^c)^+$, $\bar{\alpha}(I_2)$ converges to $\alpha - \partial_{I_1} R(0, I_2^c) > 0$ and $t(I_2)$ converges to $+\infty$.

The restriction $\Psi^l : N_{\tau_1}^s \rightarrow N_{\tau_0}^u$ of the local transition map is represented by a map $l : A_\delta^s \rightarrow A_\delta^u$, which in coordinates $(\theta, I_2) \in A_c^*$ is written as

$$(5.14) \quad \begin{aligned} l : A_c^* &\rightarrow A_c^* \\ l(\theta, I_2) &= (\theta + \Delta\theta(I_2), I_2), \end{aligned}$$

where the variation $\Delta\theta$ is given by

$$(5.15) \quad \Delta\theta(I_2) = -\bar{\omega}(I_2)t(I_2) = \frac{\bar{\omega}(I_2)}{\bar{\alpha}(I_2)} \ln \frac{f(I_2)}{\delta^2}.$$

Here

$$(5.16) \quad \bar{\omega}(I_2) = \omega + \partial_{I_2} R(f(I_2), I_2),$$

which converges to $\omega + \partial_{I_2} R(0, I_2^c) > 0$ as $I_2 \rightarrow (I_2^c)^+$. Notice that l preserves I_2 .

Since f is real-analytic and has a simple zero at $I_2^c > 0$, one can find a real-analytic function η satisfying

$$(5.17) \quad f(I_2) = (I_2 - I_2^c)\eta(I_2) \text{ with } \eta(I_2^c) \neq 0.$$

From (5.15) and (5.17) we obtain the following estimate for $\Delta\theta$

$$(5.18) \quad \Delta\theta(I_2) = \frac{\bar{\omega}(I_2)}{\bar{\alpha}(I_2)} \ln(I_2 - I_2^c) + \Lambda(I_2),$$

where

$$(5.19) \quad \Lambda(I_2) = \frac{\bar{\omega}(I_2)}{\bar{\alpha}(I_2)} \ln \frac{\eta(I_2)}{\delta^2}$$

is a real-analytic function near I_2^c . Since $f(I_2) > 0$ on A_c^* , we have that $\eta(I_2) > 0$ on this domain.

Now we use (5.18) in order to prove that the local transition map l has a monotone infinite twist near the inner boundary component S_c of the annulus A_c^* .

Lemma 5.1. *Let $\gamma : [0, 1) \rightarrow A_c^* \cup S_c$ be a real-analytic curve such that $\gamma(0) \in S_c$ and $\gamma(t) \in A_c^*$ for all $t \in (0, 1)$. Then, for all $\epsilon > 0$ sufficiently small, the curve $\{l \circ \gamma(t) : t \in (0, \epsilon)\}$ is a real-analytic spiral turning monotonically around S_c in the clockwise direction and accumulating on S_c as $t \rightarrow 0^+$. See Figure 5.2.*

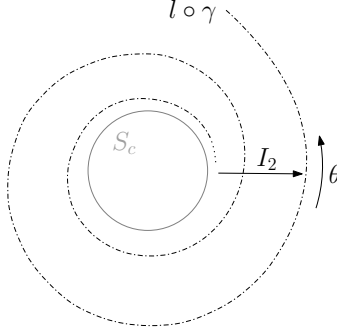


FIGURE 5.2. Infinite twist of the local transition map l near S_c .

Proof. The point $\gamma(0) \in S_c$ is represented by (θ_0, I_2^c) and the curve γ can be written as $\gamma(t) = (\theta(t), I_2(t))$, where θ and I_2 are real-analytic functions satisfying $\theta(0) = \theta_0$ and $I_2(0) = I_2^c$. Since γ is real-analytic, $\gamma(0) \in S_c$ and $\gamma(t) \in A_c^*$ for all $t \in (0, 1)$, we can find $\epsilon_0 > 0$ such that the restriction of I_2 to the interval $[0, \epsilon_0)$ is a strictly increasing function. In fact, since $I_2(t)$ is real-analytic, we have

$$I_2(t) - I_2^c = c_0 t^n + O(t^{n+1})$$

for some $c_0 > 0$, $n \in \mathbb{N}^*$ and all $t \geq 0$ small. Hence

$$I_2'(t) = nc_0 t^{n-1} + O(t^n).$$

On the other hand, (5.18) asserts that the variation $\Delta\theta$ on $\{\gamma(t), t \in (0, \epsilon_0)\}$ is given by

$$\Delta\theta(I_2(t)) = \frac{\bar{\omega}(I_2(t))}{\bar{\alpha}(I_2(t))} \ln(I_2(t) - I_2^c) + \Lambda(I_2(t)),$$

where $\Lambda(I_2(t))$ is a real-analytic function near $t = 0$. Hence

$$\begin{aligned} \frac{d}{dt}[\theta(t) + \Delta\theta(I_2(t))] &= \theta'(t) + \frac{d}{dt} \left[\frac{\bar{\omega}(I_2(t))}{\bar{\alpha}(I_2(t))} \right] \ln(I_2(t) - I_2^c) \\ &\quad + \frac{\bar{\omega}(I_2(t))}{\bar{\alpha}(I_2(t))} \frac{I_2'(t)}{I_2(t) - I_2^c} + \Lambda'(I_2(t)) I_2'(t). \end{aligned}$$

Since θ and Λ are both real-analytic near $t = 0$ and since $\frac{\bar{\omega}(I_2^c)}{\bar{\alpha}(I_2^c)} > 0$, we can find $0 < \epsilon_1 < \epsilon_0$ and a constant $c > 0$ so that

$$\frac{d}{dt}[\theta(t) + \Delta\theta(I_2(t))] > O(\ln t) + \frac{2c}{n} \frac{nc_0 t^{n-1} + O(t^n)}{c_0 t^n + O(t^{n+1})} > c \frac{1}{t} > 0$$

for all $t \in (0, \epsilon_1)$.

We conclude that $\theta(t) + \Delta\theta(I_2(t))$ decreases monotonically to $-\infty$ as $t \rightarrow 0^+$ and, therefore, the curve

$$l \circ \gamma(t) = (\theta(t) + \Delta\theta(I_2(t)), I_2(t)), t \in (0, \epsilon_1),$$

is a spiral that turns monotonically in the clockwise direction around S_c and accumulates on S_c as $t \rightarrow 0^+$. \square

6. POSITIVE TOPOLOGICAL ENTROPY

We keep using the notations established in Sections 4 and 5. Let Ψ^g and Ψ^l be the global and local symplectomorphisms defined in (4.1) and (4.2), respectively. According to Proposition 4.2, we can find $N \in \mathbb{N}$ such that $C_N^u \cap C_{\tau_1}^s \neq \emptyset$, where $C_N^u = (\Psi^g \circ \Psi^l)^{N-1} \circ \Psi^g(C_{\tau_0}^u)$, $C_{\tau_0}^u$ and $C_{\tau_1}^s$ are the intersections of $W_{\text{loc}}^u(P_{2,E})$ and $W_{\text{loc}}^s(P_{2,E})$ with D_{τ_0} and D_{τ_1} , respectively, and $0 < \tau_0 < \tau_1 < 1$, with τ_0 near 0 and τ_1 near 1.

In this section we assume that the branches of the invariant manifolds $W^u(P_{2,E})$ and $W^s(P_{2,E})$ inside S_E do not coincide. In particular, this implies that C_N^u and $C_{\tau_1}^s$ do not coincide as well. In this case, we shall prove that even if C_N^u and $C_{\tau_1}^s$ do not intersect transversely, we may consider higher iterates of the map $\Psi^g \circ \Psi^l$ in order to find infinitely many transverse intersections of $W^u(P_{2,E})$ and $W^s(P_{2,E})$ in S_E . As a consequence of these transverse intersections, we obtain infinitely many periodic orbits and infinitely many homoclinics to $P_{2,E}$ inside S_E . Moreover, the flow on $H^{-1}(E)$ has positive topological entropy. Such dynamical properties follow from the existence of an invariant subset $\Lambda_E \subset S_E$ so that the flow restricted to Λ_E semi-conjugates to a Bernoulli shift of infinite type, see [1] and [21].

As we have seen in Section 5, $(A_\#^*, A_c^*, S_c)$ is a local model for $(V_{\tau_1}^s, N_{\tau_1}^s, C_{\tau_1}^s)$ and $(V_{\tau_0}^u, N_{\tau_0}^u, C_{\tau_0}^u)$, where $A_\#^*$ is the annular neighborhood of S_c defined in (5.8), with the circle S_c defined in (5.6) being the inner boundary circle of the annulus A_c^* given in (5.7), and $V_{\tau_1}^s \subset D_{\tau_1}$, $V_{\tau_0}^u \subset D_{\tau_0}$ are, respectively, neighborhoods of the

circles $C_{\tau_1}^s$ and $C_{\tau_0}^u$, which are the inner boundary circles of the annuli $N_{\tau_1}^s$ and $N_{\tau_0}^u$ given in (5.12), respectively.

Since the Hamiltonian function H and Moser's coordinates are real-analytic, $C_N^u \cap V_{\tau_1}^s$ is represented by a real-analytic curve $\sigma_N^u \subset A_{\sharp}^*$ (possibly with many connected components) and homoclinic points in $C_N^u \cap C_{\tau_1}^s$ correspond to intersection points in $\sigma_N^u \cap S_c$.

We are assuming that C_N^u and $C_{\tau_1}^s$ intersect each other but do not coincide. It follows that each point in $\sigma_N^u \cap S_c$ is isolated since σ_N^u and S_c are real-analytic curves. Moreover, since the disks B_N^u and $B_{\tau_1}^s$ have the same symplectic area $T_{2,E} > 0$, we conclude that $C_N^u \cap N_{\tau_1}^s \neq \emptyset$ and, therefore, $\sigma_N^u \cap A_c^* \neq \emptyset$.

Definition 6.1. *We say that $p \in \sigma_N^u \cap S_c$ is a special homoclinic point if one of the following properties holds:*

- (i) *the connected component γ_p of σ_N^u containing p crosses the circle S_c at p . This means that there are points in γ_p arbitrarily close to p satisfying $I_2 < I_2^c$ and points arbitrarily close to p satisfying $I_2 > I_2^c$.*
- (ii) *σ_N^u does not contain points satisfying $I_2 < I_2^c$.*

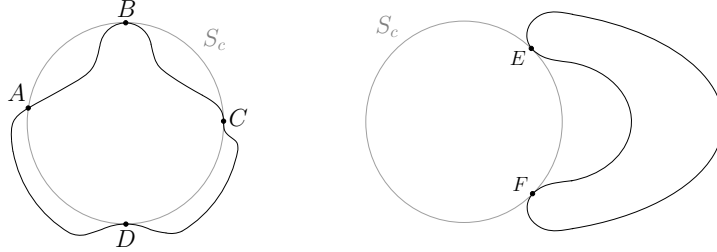


FIGURE 6.1. In this figure A , C , E and F are special homoclinic points: A and C are crossing points as in Definition 6.1 (i), and E and F are special as in Definition 6.1 (ii). The points B and D are not special homoclinic points.

We can always find a special homoclinic point $p \in \sigma_N^u \cap S_c$. In fact, if $(B_N^u \setminus C_N^u) \cap (B_{\tau_1}^s \setminus C_{\tau_1}^s) \neq \emptyset$ then a crossing point as in (i) must exist. This follows from the fact that B_N^u and $B_{\tau_1}^s$ do not coincide and have the same symplectic area $T_{2,E} > 0$. Otherwise, if $(B_N^u \setminus C_N^u) \cap (B_{\tau_1}^s \setminus C_{\tau_1}^s) = \emptyset$ then a special point as in (ii) must exist. See Figure 6.1.

Observe that since σ_N^u and S_c are real-analytic curves, either σ_N^u and S_c cross each other transversely at p or σ_N^u meets S_c tangentially at p with contact of finite order.

The dynamics near a transverse homoclinic point is very rich and rather complicated. In particular, it forces the existence of infinitely many homoclinics and infinitely many periodic orbits. This is well known since Poincaré [22], see also Smale [25].

In the following we prove that any neighborhood of a special homoclinic point (in the sense of Definition 6.1) contains infinitely many transverse homoclinic points,

as outlined by Conley^{6.1} in [3]. More specifically, we use the real-analyticity of the flow and the infinite twist of the local transition map in order to show that a special homoclinic point in $\sigma_N^u \cap S_c$ implies the existence of infinitely many transverse intersections between $(g \circ l)^N(\sigma_N^u \cap A_c^*)$ and S_c , where g and l are local representations of the global and the local transition maps Ψ^g and Ψ^l , respectively, in angle-action coordinates (θ, I_2) . For a more precise expression of g in coordinates $(x, y) = (\theta, I_2 - I_2^c)$, see the proof of Lemma 7.1 below.

Consider a special homoclinic point $p \in \sigma_N^u \cap S_c$. Let us denote by $\gamma_u \subset A_c^* \cup S_c$ a real-analytic arc contained in σ_N^u which has one end point in $p \in S_c$ and such that $\dot{\gamma}_u := \gamma_u \setminus \{p\}$ is contained in A_c^* . Observe that

$$\gamma_u \subset F^{N-1} \circ g(S_c),$$

where $F := g \circ l$.

Now let $\gamma_s \subset A_c^* \cup S_c$ be a real-analytic arc with an end point $q \in S_c$ such that $\gamma_s \setminus \{q\}$ is contained in A_c^* . Assume that γ_s satisfies

$$F^{N-1} \circ g(\gamma_s) \subset S_c \text{ and } F^{N-1} \circ g(q) = p.$$

The hypothesis of p being a special homoclinic point implies that the arcs γ_u and γ_s exist.

Using Lemma 5.1 we see that $l(\dot{\gamma}_u)$ is a real-analytic spiral turning monotonically around S_c in the clockwise direction and accumulating on S_c . Therefore, $l(\dot{\gamma}_u)$ intersects γ_s infinitely many times. Note that each of these intersections corresponds to a homoclinic orbit to $P_{2,E}$. Now we prove that such intersections are transverse near S_c .

The points $p \in \gamma_u \cap S_c$ and $q \in \gamma_s \cap S_c$ are represented in angle-action coordinates by (ϑ_p, I_2^c) and (ϑ_q, I_2^c) . We can assume that $\vartheta_p = \vartheta_q = 0$ without loss of generality. Since p is an isolated intersection point, we can write

$$\gamma_u = \{(\vartheta_{\gamma_u}(I_2), I_2) : I_2 \in [I_2^c, I_2^c + \epsilon)\}$$

for some $\epsilon > 0$ small, where ϑ_{γ_u} is a real-analytic function in $(I_2^c, I_2^c + \epsilon)$ satisfying $\vartheta_{\gamma_u}(I_2^c) = 0$. As mentioned before either σ_N^u and S_c cross each other transversely at p or they meet tangentially at p with contact of finite order. Then either $\vartheta_{\gamma_u} \equiv 0$ or ϑ_{γ_u} can be written as

$$(6.1) \quad \vartheta_{\gamma_u}(I_2) = (I_2 - I_2^c)^n \beta(I_2),$$

where β is a real-analytic function satisfying $\beta(I_2^c) \neq 0$, $a \geq 0$ and $n > 0$ is either an integer in case the intersection is transverse or $n = \frac{1}{k}$ for an integer $k > 0$ in case the intersection is tangential with contact of finite order.

As we have seen in Section 5, the local transition map $l : A_c^* \rightarrow A_c^*$ is defined by $l(\theta, I_2) = (\theta + \Delta\theta(I_2), I_2)$, where the variation $\Delta\theta(I_2)$ is given in (5.18). Thus, the real-analytic curve $l(\dot{\gamma}_u)$ assumes the following form

$$l(\dot{\gamma}_u) = \{(\vartheta_{l(\dot{\gamma}_u)}(I_2) := \vartheta_{\gamma_u}(I_2) + \Delta\theta(I_2), I_2) : I_2 \in (I_2^c, I_2^c + \epsilon)\}.$$

From (5.18) and (6.1) we obtain, for $I_2 - I_2^c > 0$ small,

$$\vartheta_{l(\dot{\gamma}_u)}(I_2) = (I_2 - I_2^c)^n \beta(I_2) + \frac{\bar{\omega}(I_2)}{\bar{\alpha}(I_2)} \ln(I_2 - I_2^c) + \Lambda(I_2),$$

^{6.1}Churchill and Rod also addressed this question in a more general setup, see [2, Theorem 1.1, Remark 1.8 (b) and (c)].

where $\Lambda(I_2)$ is a real-analytic function near I_2^c . It follows that

$$\begin{aligned} \frac{d\vartheta_{l(\dot{\gamma}_u)}}{dI_2}(I_2) &= n(I_2 - I_2^c)^{n-1}\beta(I_2) + (I_2 - I_2^c)^n\beta'(I_2) \\ &\quad + \frac{\bar{\omega}(I_2)}{\bar{\alpha}(I_2)} \frac{1}{I_2 - I_2^c} + \partial_{I_2} \left(\frac{\bar{\omega}(I_2)}{\bar{\alpha}(I_2)} \right) \ln(I_2 - I_2^c) + \Lambda'(I_2). \end{aligned}$$

Hence, in both cases $n \in \mathbb{N}^*$ or $n = \frac{1}{k}$ with $k \in \mathbb{N}^*$, we find a constant $c_1 > 0$ so that

$$(6.2) \quad \frac{d\vartheta_{l(\dot{\gamma}_u)}}{dI_2}(I_2) > c_1 \frac{1}{I_2 - I_2^c}$$

for all $I_2 - I_2^c > 0$ sufficiently small. Inequality (6.2) also holds in the case $\vartheta_{\gamma_u} \equiv 0$.

Now let $\vartheta_{\gamma_s}(I_2)$ be a function (real-analytic in $(I_2^c, I_2^c + \epsilon)$) determined by γ_s as follows

$$\gamma_s = \{(\vartheta_{\gamma_s}(I_2), I_2) : I_2 \in [I_2^c, I_2^c + \epsilon)\},$$

where $\vartheta_{\gamma_s}(I_2^c) = 0$. As before, either $\vartheta_{\gamma_s} \equiv 0$ or ϑ_{γ_s} can be written as

$$(6.3) \quad \vartheta_{\gamma_s}(I_2) = (I_2 - I_2^c)^m \varsigma(I_2),$$

where ς is a real-analytic function satisfying $\varsigma(I_2^c) \neq 0$ and $m > 0$ is either an integer or assumes the form $m = \frac{1}{j}$ for some integer $j > 1$, depending on the way γ_s meets S_c at the point q . In both cases we can choose $\lambda \in (0, 1)$ so that

$$(6.4) \quad \frac{d\vartheta_{\gamma_s}}{dI_2}(I_2) = m(I_2 - I_2^c)^{m-1}\varsigma(I_2) + (I_2 - I_2^c)^m\varsigma'(I_2) < c_1 \frac{1}{(I_2 - I_2^c)^{1-\lambda}},$$

for all $I_2 - I_2^c > 0$ small. Inequality above also holds in the case $\vartheta_{\gamma_s} \equiv 0$.

Using (6.2) and (6.4) we conclude

$$\frac{d\vartheta_{l(\dot{\gamma}_u)}}{dI_2}(I_2) > \frac{d\vartheta_{\gamma_s}}{dI_2}(I_2)$$

for all $I_2 > I_2^c$ near I_2^c , proving that $l(\dot{\gamma}_u)$ intersects γ_s transversely at infinitely many points approaching $(\theta, I_2) = (0, I_2^c)$. See Figure 6.2.

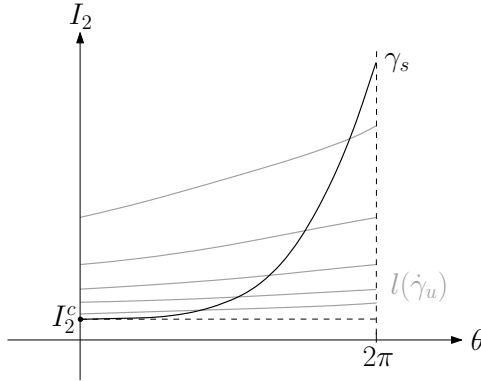


FIGURE 6.2. Representation of the curves $l(\dot{\gamma}_u)$ and γ_s in angle-action coordinates (θ, I_2) .

Transverse intersection points between $l(\dot{\gamma}_u)$ and γ_s correspond to transverse homoclinic orbits to $P_{2,E}$. Therefore we have proved that $P_{2,E}$ admits infinitely

many transverse homoclinic orbits in \dot{S}_E . It is well known that the existence of a transverse homoclinic orbit implies infinitely many nearby periodic orbits and positivity of topological entropy. See [21, Chapter III] for a discussion of this result and other interesting dynamical properties implied by the transverse homoclinic orbits such as the existence of an invariant subset of \dot{S}_E so that the flow restricted to it is semi-conjugated to a Bernoulli shift with infinitely many symbols.

7. AREA PRESERVING HOMEOMORPHISMS OF THE OPEN ANNULUS

Now we deal with the case where the branches of $W^s(P_{2,E})$ and $W^u(P_{2,E})$ inside S_E coincide. In this situation the circles $C_N^u = \Psi^{N-1} \circ \Psi^g(C_{\tau_0}^u)$ and $C_{\tau_1}^s$ coincide in D_{τ_1} , where $N \in \mathbb{N}^*$ is as in Proposition 4.2. Once again we follow notations established in Sections 4 and 5. It immediately follows that $P_{2,E}$ admits infinitely many homoclinics in \dot{S}_E . Moreover, in this case the Hamiltonian flow defines a symplectomorphism $\Psi : \mathcal{A} \rightarrow \mathcal{A}$, where $\Psi := \Psi^g \circ \Psi^l$ and \mathcal{A} consists of D_{τ_1} with N disjoint closed disks removed

$$\mathcal{A} := D_{\tau_1} \setminus \bigcup_{j=0}^{N-1} \Psi^{-j}(B_{\tau_1}^s).$$

Note that the assumption $C_N^u = C_{\tau_1}^s$ implies that $\Psi^{-j}(B_{\tau_1}^s) = \Psi^{N-1-j} \circ \Psi^g(B_{\tau_0}^u)$ for all $j = 0, \dots, N-1$. The map Ψ describes the dynamics on an invariant open subset $\mathcal{U}_{\mathcal{A}} \subset \dot{S}_E$, which is given by the trajectories in \dot{S}_E intersecting \mathcal{A} transversely. Thus the Hamiltonian flow restricted to $\mathcal{U}_{\mathcal{A}}$ admits \mathcal{A} as a global surface of section where Ψ is the first return map. Observe that Ψ preserves the outer boundary component of \mathcal{A} (corresponding to the binding $P_{3,E}$), i.e., Ψ maps points close to $P_{3,E}$ into points close to $P_{3,E}$. The inner boundary components of \mathcal{A} are permuted by Ψ .

Using results due to J. Franks on area preserving homeomorphisms of the open annulus [9, 10, 11], we shall prove that $\Psi : \mathcal{A} \rightarrow \mathcal{A}$ has infinitely many periodic points, which correspond to infinitely many periodic orbits of the Hamiltonian flow in \dot{S}_E .

We start by defining the following equivalence relation in D_{τ_1} :

$$x \sim y \Leftrightarrow \exists j \in \{0, \dots, N-1\} \text{ s.t. } x, y \in \Psi^{-j}(B_{\tau_1}^s).$$

In this way we obtain an open disk $\tilde{D}_1 := D_{\tau_1}/\sim$ whose topology is induced by the natural projection $\Pi : D_{\tau_1} \rightarrow \tilde{D}_1$. Observe that Π collapses the closed disks $\Psi^{-j}(B_{\tau_1}^s) \subset D_{\tau_1}$ into distinct points $p_j \in \tilde{D}_1$, $j = 0, \dots, N-1$. Notice also that $\Pi|_{\mathcal{A}}$ is a bijection onto $\tilde{D}_1 \setminus \{p_0, \dots, p_{N-1}\}$ and hence $\Pi(\mathcal{A})$ admits a natural smooth structure so that $\Pi|_{\mathcal{A}}$ is a smooth diffeomorphism onto $\Pi(\mathcal{A})$. Consider the finite area form ω_1 on $\Pi(\mathcal{A}) = \tilde{D}_1 \setminus \{p_0, \dots, p_{N-1}\}$ induced by $(\Pi|_{\mathcal{A}})_*\omega_0$, where ω_0 is the symplectic form on D_{τ_1} induced by the ambient symplectic structure. Using Π and the symplectomorphism $\Psi : \mathcal{A} \rightarrow \mathcal{A}$ we obtain an area preserving homeomorphism $\Phi : \tilde{D}_1 \rightarrow \tilde{D}_1$ defined on $\Pi(\mathcal{A})$ by $\Phi = \Pi \circ \Psi \circ \Pi^{-1}$ and by declaring that $\Phi(p_j) = p_{j-1}$, $\forall j = 1, \dots, N-1$ and $\Phi(p_0) = p_{N-1}$. The area form ω_1 naturally extends to a finite area form on \tilde{D}_1 which is Φ -invariant.

Let us first assume that $N > 1$. Note that Φ must have a fixed point $\bar{p} \notin \{p_0, \dots, p_{N-1}\}$ and $\Phi|_{\tilde{D}_1 \setminus \{\bar{p}\}}$ is an area preserving homeomorphism of the open annulus (homotopic to the identity) with a periodic orbit $\{p_0, \dots, p_{N-1}\}$. In this

case we can directly apply Franks' theorem in [10] to conclude that Φ has infinitely many periodic points in \tilde{D}_1 which implies that the Hamiltonian flow admits infinitely many periodic orbits in $\mathcal{U}_A \subset \dot{S}_E$.

Now let us assume $N = 1$. In this case \mathcal{A} is given by the open annulus

$$D_{\tau_1} \setminus B_{\tau_1}^s \simeq (\mathbb{R}/2\pi\mathbb{Z}) \times (0, 1)$$

and the symplectomorphism $\Psi = \Psi^g \circ \Psi^l : \mathcal{A} \rightarrow \mathcal{A}$ can be seen as a diffeomorphism of $(\mathbb{R}/2\pi\mathbb{Z}) \times (0, 1)$ preserving a finite area form. Recall the local model (A_c^*, S_c) for $(N_{\tau_1}^s, C_{\tau_1}^s)$, where S_c and A_c^* are defined in (5.6) and (5.7), respectively, and $N_{\tau_1}^s \subset D_{\tau_1} \setminus B_{\tau_1}^s$ is defined in (5.12). In angle-action coordinates (θ, I_2) , S_c is represented by $\{I_2 = I_2^c\}$, where $I_2^c > 0$ is such that $f(I_2^c) = 0$, see (5.3). Observe that $(\theta, I_2 - I_2^c) \in (\mathbb{R}/2\pi\mathbb{Z}) \times (0, \epsilon)$, with $\epsilon > 0$ sufficiently small, can be used as coordinates in \mathcal{A} near its inner boundary component $C_{\tau_1}^s$ via the identifications above.

Let $\pi : \mathbb{R} \times (0, 1) \rightarrow (\mathbb{R}/2\pi\mathbb{Z}) \times (0, 1)$ be the universal covering map

$$(7.1) \quad \pi(x, y) = (x \bmod 2\pi, y), \forall (x, y) \in \mathbb{R} \times (0, 1).$$

With the identification above, we have

$$(x, y) = (\theta, I_2 - I_2^c), \forall (x, y) \in \mathbb{R} \times (0, \epsilon),$$

where (θ, I_2) are the angle-action coordinates and θ is now viewed as \mathbb{R} -valued.

Let $\tilde{\Psi} : \mathbb{R} \times (0, 1) \rightarrow \mathbb{R} \times (0, 1)$ be a lift of Ψ with respect to π . The infinite twist behavior of the local transition map proved in Lemma 5.1 implies that $\tilde{\Psi}$ also has an infinite twist near the lower boundary component $\mathbb{R} \times \{0\}$, as we show in the following lemma.

Lemma 7.1. *There exist $0 < \epsilon' < \epsilon$ and real-analytic functions $\Theta_1(x)$, defined in \mathbb{R} , $H_1(x, y)$ and $H_2(x, y) > 0$, defined in $\mathbb{R} \times (-\epsilon', \epsilon')$, all of them 2π -periodic in x , such that, denoting $(\tilde{x}(x, y), \tilde{y}(x, y)) = \tilde{\Psi}(x, y)$, we have*

$$(7.2) \quad \begin{aligned} \tilde{x}(x, y) &= x + \Delta(y) + \Theta_1(x + \Delta(y)) + yH_1(x + \Delta(y), y), \\ \tilde{y}(x, y) &= yH_2(x + \Delta(y), y), \end{aligned}$$

for all $(x, y) \in \mathbb{R} \times (0, \epsilon')$, where

$$(7.3) \quad \Delta(y) := \frac{\bar{\omega}(y + I_2^c)}{\bar{\alpha}(y + I_2^c)} \ln y + \Lambda(y + I_2^c),$$

and $\bar{\alpha}, \bar{\omega}$ and Λ are real-analytic functions defined in (5.13), (5.16) and (5.19), respectively. Moreover, $\tilde{\Psi}$ satisfies the following infinite twist property near $\mathbb{R} \times \{0\}$: fixing a bounded subset $B \subset \mathbb{R}$, we have

$$\tilde{x}(x, y) \rightarrow -\infty \text{ and } \tilde{y}(x, y) \rightarrow 0^+, \text{ as } y \rightarrow 0^+,$$

uniformly for $x \in B$.

Proof. Recall that the local transition map l is given by

$$l(\theta, I_2) = \left(\theta + \frac{\bar{\omega}(I_2)}{\bar{\alpha}(I_2)} \ln(I_2 - I_2^c) + \Lambda(I_2), I_2 \right),$$

where $\bar{\alpha}, \bar{\omega}$ and Λ are real-analytic functions given by (5.13), (5.16) and (5.19), respectively.

In the strip $\mathbb{R} \times (0, \epsilon)$, a point (x, y) coincides with the angle-action coordinates $(\theta, I_2 - I_2^c)$ and $\tilde{\Psi}$ splits as $\tilde{\Psi} = \tilde{g} \circ \tilde{l}$, where \tilde{g} and \tilde{l} are lifts of the global and

local transition maps, respectively, with respect to the universal covering map π , see (7.1). In coordinates (x, y) , a choice of \tilde{l} is written as

$$(7.4) \quad \tilde{l}(x, y) = (x + \Delta(y), y), \forall (x, y) \in \mathbb{R} \times (0, \epsilon),$$

with $\Delta(y)$ defined in (7.3).

Let us denote

$$(7.5) \quad \tilde{g}(x, y) = (X(x, y), Y(x, y)),$$

where X and Y are real-analytic functions defined in $\mathbb{R} \times (-\epsilon, \epsilon)$. Since we are assuming $N = 1$, and therefore $\Psi^g(C_{\tau_0}^u) = C_{\tau_1}^s$, the global transition map g leaves the boundary component $S_c = \{I_2 = I_2^c\}$ invariant. Then $Y(x, 0) = 0$ for all $x \in \mathbb{R}$ and there exists a real-analytic function $H_2 : \mathbb{R} \times (-\epsilon, \epsilon) \rightarrow \mathbb{R}$, 2π -periodic in x , so that $Y(x, y) = y^k H_2(x, y)$ for some integer $k > 0$ and $H_2(x, 0) \neq 0$ for all $x \in \mathbb{R}$. We claim that $k = 1$. In fact, since \tilde{g} is an area preserving diffeomorphism, we have

$$(7.6) \quad \det \begin{pmatrix} \partial_x X & \partial_y X \\ \partial_x Y & \partial_y Y \end{pmatrix} = 1.$$

Observe that $\partial_x Y(x, 0) = 0$ for all x . Since $\partial_y Y = ky^{k-1}H_2(x, y) + y^k \partial_y H_2(x, y)$ and $\partial_y Y(x, 0) \neq 0, \forall x \in \mathbb{R}$, we must have $k = 1$. Thus

$$(7.7) \quad Y(x, y) = yH_2(x, y), \forall (x, y) \in \mathbb{R} \times (-\epsilon, \epsilon).$$

Using that $\partial_y Y(x, 0) > 0$, we obtain $H_2(x, 0) > 0$ for all $x \in \mathbb{R}$. This implies the existence of $0 < \epsilon' < \epsilon$ so that $H_2(x, y) > 0$ for all $(x, y) \in \mathbb{R} \times (-\epsilon', \epsilon')$.

We can take $\epsilon' > 0$ even smaller so that $X(x, y) = X(x, 0) + yH_1(x, y)$, where $H_1(x, y)$ is a real-analytic function defined in $\mathbb{R} \times (-\epsilon', \epsilon')$, which is 2π -periodic in x . Let Θ_1 be the real-analytic function given by $\Theta_1(x) = X(x, 0) - x, \forall x \in \mathbb{R}$. Note that Θ_1 is 2π -periodic. Then we write

$$(7.8) \quad X(x, y) = x + \Theta_1(x) + yH_1(x, y), \forall (x, y) \in \mathbb{R} \times (-\epsilon', \epsilon').$$

Now denoting $(\tilde{x}, \tilde{y}) = \tilde{g} \circ \tilde{l}$, we finally obtain (7.2) from (7.4), (7.5), (7.7) and (7.8). Since $\Delta(y) \rightarrow -\infty$ as $y \rightarrow 0^+$ and $\Theta_1(x), H_1(x, y)$ and $H_2(x, y) > 0$ are bounded, we conclude from (7.2) that $\tilde{x}(x, y) \rightarrow -\infty$ and $\tilde{y}(x, y) \rightarrow 0^+$ as $y \rightarrow 0^+$ for all $x \in \mathbb{R}$. Clearly, this convergence is uniform in x , if x lies in a bounded subset $B \subset \mathbb{R}$, since Θ_1 and H_1 are bounded. \square

For each $k \in \mathbb{N}$, consider the lift $\tilde{\Psi}_k : \mathbb{R} \times (0, 1) \rightarrow \mathbb{R} \times (0, 1)$ of Ψ given by

$$(7.9) \quad \tilde{\Psi}_k(x, y) = \tilde{\Psi}(x, y) + (2k\pi, 0).$$

We shall see that the infinite twist of $\tilde{\Psi}$ near $\mathbb{R} \times \{0\}$ implies the existence of a fixed point for $\tilde{\Psi}_k$ for each k sufficiently large. In order to do that, we first recall the notion of returning disks introduced by J. Franks in [9].

Definition 7.2 (J. Franks [9]). *Let f be a homeomorphism of the open annulus $A := (\mathbb{R}/2\pi\mathbb{Z}) \times (0, 1)$, which is homotopic to the identity map. Let \tilde{f} be a lift of f to $\tilde{A} := \mathbb{R} \times (0, 1)$ with respect to the covering map π defined in (7.1). We say that an open disk $U \subset \tilde{A}$ is a positively returning disk for \tilde{f} if*

- (i) $\tilde{f}(U) \cap U = \emptyset$,
- (ii) *there exists an integer $n > 0$ so that $\tilde{f}^n(U) \cap (U + m) \neq \emptyset$ for some $m > 0$, where $U + m := \{(x + m, y) : (x, y) \in U\}$.*

Similarly, we define negatively returning disks for \tilde{f} by requiring $m < 0$ in (ii).

The following result proved by Franks in [9] (see also [11]) provides at least one fixed point for a lift of an area preserving homeomorphism of the open annulus containing both negatively and positively returning disks.

Theorem 7.3 (J. Franks [9, 11]). *Let $f : A \rightarrow A$ be a homeomorphism of the open annulus $A = (\mathbb{R}/2\pi\mathbb{Z}) \times (0, 1)$ which is homotopic to the identity map and preserves a finite area form. Let $\tilde{f} : \tilde{A} \rightarrow \tilde{A}$ be a lift of f to the universal covering space $\tilde{A} = \mathbb{R} \times (0, 1)$ with respect to the covering map π defined in (7.1). Assume that \tilde{f} admits both positively and negatively returning disks, which are lifts of disks in A . Then \tilde{f} has a fixed point.*

The proof of Theorem 7.3 is contained in the proof of the more general Theorem 2.1 in [9], see also [11].

Proposition 7.4 below asserts that Ψ admits infinitely many fixed points. Its proof consists of showing that $\tilde{\Psi}_k$ admits both positively and negatively returning disks, which are lifts of disks, for every $k > 0$ sufficiently large. As a consequence of Theorem 7.3, we obtain a fixed point for $\tilde{\Psi}_k$ for each k sufficiently large. Observe that fixed points of $\tilde{\Psi}_{k_1}$ and $\tilde{\Psi}_{k_2}$, with $k_1 \neq k_2$, project into distinct fixed points of Ψ . Therefore, we derive infinitely many fixed points for Ψ .

Proposition 7.4. *Ψ has infinitely many fixed points.*

Proof. We can assume that $\tilde{\Psi}(x, y) = (\tilde{x}(x, y), \tilde{y}(x, y))$, $\forall (x, y) \in \mathbb{R} \times (0, \epsilon')$, where \tilde{x}, \tilde{y} and $\epsilon' > 0$ are given in Lemma 7.1, see equation (7.2).

Define the open disk $Q_\mu^+ \subset \mathbb{R} \times (0, \epsilon')$ depending on a small parameter $0 < \mu < \frac{\epsilon'}{2}$ as follows

$$Q_\mu^+ := (0, 2\pi) \times \left(\mu, \frac{\epsilon'}{2}\right).$$

Using that $\tilde{x}(x, y) \rightarrow -\infty$ and $\tilde{y}(x, y) \rightarrow 0^+$ as $y \rightarrow 0^+$, for all fixed x , we find $l_0 \in \mathbb{Z}$, so that $\tilde{\Psi}(Q_\mu^+) \cap (Q_\mu^+ + 2l_0\pi) \neq \emptyset$, for all $\mu > 0$ sufficiently small. Fixing such a small $\mu > 0$ and using that $\tilde{\Psi}(Q_\mu^+)$ is a bounded subset of $\mathbb{R} \times (0, 1)$, we obtain that $\tilde{\Psi}_k(Q_\mu^+)$ does not intersect Q_μ^+ for all $k \in \mathbb{N}$ sufficiently large. Now since $\tilde{\Psi}_k(Q_\mu^+)$ intersects $Q_\mu^+ + 2(l_0 + k)\pi$ we conclude that Q_μ^+ is a positively returning disk for $\tilde{\Psi}_k$ for all $k \in \mathbb{N}$ large. See Figure 7.1.

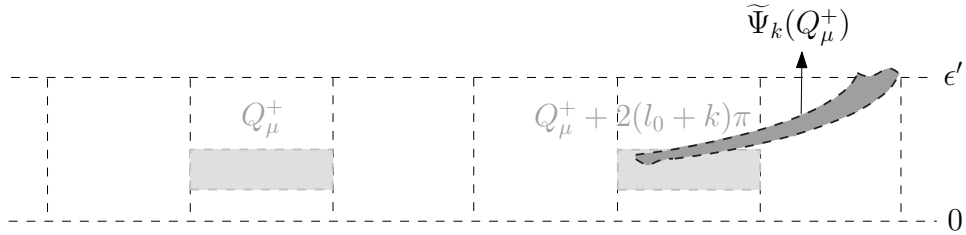


FIGURE 7.1. Positively returning disk Q_μ^+ for $\tilde{\Psi}_k$.

Now for each fixed $k \in \mathbb{N}$, let $Q_k^- \subset \mathbb{R} \times (0, \epsilon')$ be the open disk given by

$$Q_k^- := (0, 2\pi) \times (0, \epsilon_k),$$

where $0 < \varepsilon_k \ll \mu$ is to be determined below and μ is fixed as above. Using that $\tilde{x}(x, y) \rightarrow -\infty$ and $\tilde{y}(x, y) \rightarrow 0^+$ as $y \rightarrow 0^+$, uniformly in $x \in (0, 2\pi)$, we obtain $\varepsilon_k > 0$ small so that $\tilde{\Psi}(Q_k^-) \cap (Q_k^- - 2k\pi) = \emptyset$. Moreover, $\tilde{\Psi}(Q_k^-) \cap (Q_k^- - 2l\pi) \neq \emptyset$ for all $l \in \mathbb{N}$ sufficiently large. Fixing one such $\varepsilon_k > 0$ small, we conclude that $\tilde{\Psi}_k(Q_k^-) \cap Q_k^- = \emptyset$ and that $\tilde{\Psi}_k(Q_k^-) \cap (Q_k^- - 2(l-k)\pi) \neq \emptyset$ for every large l . It follows that Q_k^- is a negatively returning disk for $\tilde{\Psi}_k$, see Figure 7.2.

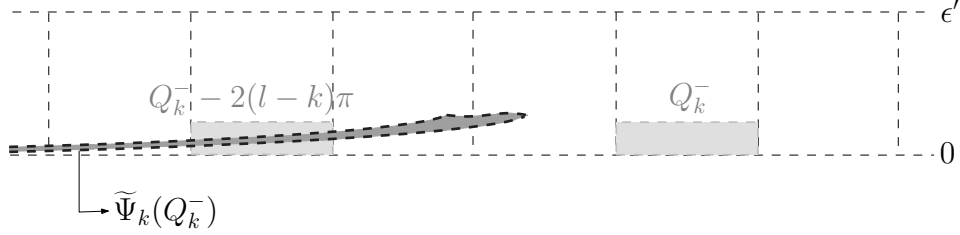


FIGURE 7.2. Negatively returning disk Q_k^- for $\tilde{\Psi}_k$.

We conclude that for all $k \in \mathbb{N}$ sufficiently large, $\tilde{\Psi}_k$ admits both positively and negatively returning disks in $\mathbb{R} \times (0, 1)$, which are both lifts of disks in $(\mathbb{R}/2\pi\mathbb{Z}) \times (0, 1)$. Theorem 7.3 implies that $\tilde{\Psi}_k$ has a fixed point $q_k \in \mathbb{R} \times (0, 1)$. Clearly $\pi(q_k) \in (\mathbb{R}/2\pi\mathbb{Z}) \times (0, 1)$ is a fixed point of Ψ . Using (7.9) we see that q_k is not a fixed point of $\tilde{\Psi}_j$ if $j \neq k$ and hence $\pi(q_j) \neq \pi(q_k)$ if $j \neq k$. This implies that Ψ has infinitely many fixed points. \square

Finally observe that each fixed point of the first return map $\Psi : \mathcal{A} \subset D_{\tau_1} \rightarrow \mathcal{A}$ obtained in Proposition 7.4 corresponds to a periodic orbit of the Hamiltonian flow inside $\mathcal{U}_{\mathcal{A}} \subset \dot{S}_E$. Hence \dot{S}_E contains infinitely many periodic orbits and infinitely many homoclinic orbits to $P_{2,E}$ in case the branches of $W_E^s(P_{2,E})$ and $W_E^u(P_{2,E})$ in S_E coincide.

Acknowledgements. NP was partially supported by FAPESP 2014/08113-1. PS was partially supported by CNPq 306106/2016-7 and by FAPESP 2016/25053-8.

REFERENCES

- [1] P. Bernard, C. Grotta-Ragazzo and P. Salomão. *Homoclinic orbits near saddle-center fixed points of Hamiltonian systems with two degrees of freedom*, Astérisque, **286** (2003), 151–165.
- [2] R. C. Churchill and D. L. Rod. *Pathology in dynamical systems. III. Analytic Hamiltonians*. Journal of Differential Equations 37.1 (1980): 23–38.
- [3] C. Conley. *Twist mappings, linking, analyticity, and periodic solutions which pass close to an unstable periodic solution*. Topological dynamics (1968): 129–153.
- [4] A. Chakraborty, S. Bagchi, and K. L. Sebastian, J. Comput. Theor. Nanosci. **4**, 504 (2007).
- [5] P. Collins, G.S. Ezra, S. Wiggins. *Isomerization dynamics of a buckled nanobeam*. Physical Review E **86**, (2012).
- [6] D. Delatte. *On normal forms in Hamiltonian dynamics, a new approach to some convergence questions*. Erg. Th. Dyn. Sys., **15**, (1995), 49–66.
- [7] H.R. Dullin, M. Horányi, J.E. Howard. *Generalizations of the Störmer problem for dust grain orbits*. Physica D **171**, (2002), 178–195.
- [8] N. de Paulo and P. Salomão. *Systems of transversal sections near critical energy levels of Hamiltonian systems in \mathbb{R}^4* , to appear in Memoirs of AMS.

- [9] J. Franks. *Generalizations of the Poincaré-Birkhoff theorem*. Ann. of Math. **128** (1988), 139–151.
- [10] J. Franks. *Area preserving homeomorphisms of open surfaces of genus zero*. New York J. Math. 2.1 (1996): 19.
- [11] J. Franks. *Erratum to “Generalizations of the Poincaré-Birkhoff theorem”*. Ann. of Math. **164** (2006), 1097–1098.
- [12] G. Fusco, G. F. Gronchi and M. Novaga. *On the existence of connecting orbits for critical values of the energy*. arXiv preprint arXiv:1701.07514 (2017).
- [13] G. Fusco, G. F. Gronchi and M. Novaga. *On the existence of heteroclinic connections*. To appear in São Paulo Journal of Math. Sci, 2017.
- [14] C. Grotta-Ragazzo, M. Kulesza and Pedro A. S. Salomão. *Equatorial dynamics of charged particles in planetary magnetospheres*. Physica D: Nonlinear Phenomena, Volume 225, Issue 2, (2007), 169–183.
- [15] H. Hofer, K. Wysocki and E. Zehnder. *The dynamics of strictly convex energy surfaces in \mathbb{R}^4* . Ann. of Math. **148** (1998), 197–289.
- [16] H. Hofer, K. Wysocki and E. Zehnder. *Finite energy foliations of tight three-spheres and Hamiltonian dynamics*. Ann. Math **157** (2003), 125–255.
- [17] J.E. Howard, M. Horanyi, G.R. Stewart. *Global dynamics of charged dust particles in planetary magnetospheres*. Phys. Rev. Lett. 83 (20), 3993–3996 (1999).
- [18] U. Hryniewicz and P. Salomão. *On the existence of disk-like global sections for Reeb flows on the tight 3-sphere*. Duke Mathematical Journal **160**, 3 (2011), 415–465.
- [19] D. A. Mendis, J. R. Hill, H. Houpis. *Charged dust in Saturn’s magnetosphere*. Journal of Geophysical Research: Solid Earth 88.S02 (1983).
- [20] J. Moser. *On the generalization of a theorem of A. Liapounoff*. Communications on Pure and Applied Mathematics, **11**, 2 (1958), 257–271.
- [21] J. Moser. *Stable and random motions in dynamical systems: With special emphasis on celestial mechanics*. Ann. Math. Stud. 77, Princeton University Press, (1973).
- [22] H. Poincaré. *Les Méthodes Nouvelles de la Mécanique Céleste*. New York: Dover Publications (reprint), (1957).
- [23] H. Rüssmann, *Über das Verhalten analytischer Hamiltonscher differentialgleichungen in der Nähe einer Gleichgewichtslösung*, Math. Ann., Princeton University Press, **154**, (1964), 285–300.
- [24] P. Salomão. *Convex energy levels of Hamiltonian systems*. Qualitative Theory of Dynamical Systems **4**, 2, (2004), 439–454.
- [25] S. Smale. *Diffeomorphisms with many periodic points*. Differential and Combinatorial Topology. Cairnes, S.S. (ed.) (1965), Princeton, NJ: Princeton University Press, pp. 63–80.
- [26] J. Xu, X. Wu, D. Z. Ma. *Chaotic motion of dust particles in planetary magnetospheres*. Pramana **74** (6), (2010), 907–917.

(Naiara V. de Paulo) UNIVERSIDADE FEDERAL DE SANTA CATARINA, DEPARTAMENTO DE MATEMÁTICA – RUA POMERODE, 710 - SALTO DO NORTE - BLUMENAU SC, BRAZIL 89065-300.

E-mail address: naiara.vergiani@ufsc.br

(Pedro A. S. Salomão) UNIVERSIDADE DE SÃO PAULO, INSTITUTO DE MATEMÁTICA E ESTATÍSTICA – DEPARTAMENTO DE MATEMÁTICA, RUA DO MATÃO, 1010 - CIDADE UNIVERSITÁRIA - SÃO PAULO SP, BRAZIL 05508-090.

E-mail address: psalomao@ime.usp.br